Mapping the relationship between integrin activation, focal adhesion organization and mechanotransduction in fibroblasts

Valeriia Grudtsyna
2021

Master's Thesis in
Biomedical Engineering

Assistant supervisor: Vinay Swaminathan
Principal supervisor: Per Augustsson
Examiner: Thomas Laurell

Faculty of Engineering LTH
Department of Biomedical Engineering

1 Abstract

Cells can sense and respond to mechanical forces through a process called mechanotransduction. It is controlled by the mechanical cues, originated from the cell's microenvironment, and occurs via a complex, step-wise process. In this process, a cascade of events occurs, where the forces are essentially sensed by integrins and transmitted through filamentous actin (F-actin). The downstream events lead to the activation of transcriptional factors, which in turn impact the cellular response. YAP is a transcriptional coregulator, involved in cell proliferation. It is controlled by the canonical Hippo signaling pathway together with the mechanotransduction pathway. The effect of the latter is less studied and the exact process is yet unknown.

This thesis focuses on further investigations of the mechanotransduction pathway and its influence on YAP activation in fibroblasts. Different microenvironments were modulated by modifying the fibronectin (FN) coating, which controls the amount of integrin activation and consequently affects the FA morphology together with the organization of F-actin. The organizational degree of F-actin in focal adhesions (FA) and morphological FA properties were compared to the YAP response. The results revealed that YAP activation is increased proportionally to the FN concentration, correlating to F-actin data. However, the lowest FN concentration caused a non-matching increase of activation. The findings propose that the YAP response might to some extent be determined by integrin activation. However, it has yet been impossible to decouple the effect of the Hippo signaling.

2 Acknowledgements

I would like to express my huge gratitude to Vinay Swaminathan and the whole LCMM lab, who made this project not only possible but fruitful and unforgettable. With your help, I have been able to explore the dungeons of cell biology and dive into the unpredictable world, called science. Thank you, everyone, for letting me be a part of such a great team!

This thesis was performed at the laboratory of cell and molecular mechanobiology (LCMM), BMC. Vinay Swaminathan designed this project and provided me with valuable information and discussions. Swathi Packirisamy helped me to prepare the samples and taught me immunostaining together with other biological techniques. Wesley Sturgess reviewed this report and was always there to help. Aravindh Subramani cheered us all up. I also like to thank my supervisor Per Augustsson for guidance and for supplying me with practical information.

3 Populärvetenskaplig sammanfattning

Cancer är ett existentiellt problem världen runt. Den kan uppstå i nästan vilken vävnad som helst och innebär att vissa celler börjar dela sig obehindrat. Dessutom kan tumörceller sprida sig till andra delar av kroppen och bilda så kallade metastaser. Ibland räcker det att lokalt ökad styvhet bidrar till cancercellernas metastasering och på det sättet förvärrar sjukdomen. Därför är det väldigt viktigt att undersöka i grunden vad som kan generara en sådan respons och granska processer som sker inuti cellen.

I detta projekt vill vi undersöka hur specifika proteiner, nämligen Yes-assocoiated protein (YAP) och aktinfilament, påverkar varandra. YAP är involverad i cellens transkriptionsprocess, där cellen bestämmer vilka gener i DNAt som ska översättas till mRNA och därmed börja tillverka proteiner som kommer hjälpa cellen att anpassa sig till sin omgivning. När YAP är i sin aktiva form pendlar den in i cellkärnan där den kan initiera DNA-transkription. YAP är inaktiverat, då den är lokaliserad i cytoplasman. YAP är bland annat reglerad av så kallad Hippo cellsignalering som kontrollerar organstorleken genom att bestämma ifall en cell ska dela sig eller begå apoptos (programmerad celldöd). Ifall dessa funktioner ej fungerar korrekt, kan det leda till sjukdomar som exempelvis cancer. Därför är regleringen av YAP väldigt intressant för forskningen. Det finns belägg för att Hippo cellsignaleringen inte är det enda som reglerar YAP, utan att det också kan styras av de mekaniska signalerna utifrån. Det finns olika teorier om hur det kan ske och i detta projekt tittar vi närmare på en av dem.

Celler bildar fysiska länkar tvärs över cellmembranet som kopplar dem till omgivningen. Genom dessa länkar kan de mekaniska signalerna först kännas av och därefter färdas vidare. Via en kedjereaktion kan de nå cellkärnan och generera specifik respons. Dessa länkar kallas för fokaladhesioner och är uppbyggda av många olika proteiner. De transmembrana proteinerna som binder till den extracellulära matrisen (ECM) kallar för integriner. Det existerar många slags integriner som kan binda till respektive ECM-markörer. De långa filamentstrukturerna som till största del utgör cellens skelett och tjänar som signalöverförare kallas för aktin. Aktinnätverket är kopplat till fokaladhesionerna och spinner hela cellens cytosol.

I detta projekt söktes en koppling mellan organiseringen av aktinet i fokaladhesionerna och YAP-aktiveringen. Vi utvecklade därför två experiment. Vi tar reda på graden av aktinorganisering (hur pass slumpmässigt filamenten är ordnade) genom att färga in aktinet och sedan avbilda med ett polarisationskänsligt mikroskop som endast skannar de ytliga strukturer på cellen. Sedan, med hjälp av bildanalys, har bilddatan kunnat sammanställas till lätthanterliga värden. För att undersöka YAP-aktivering, färgade vi på liknande sätt in YAP, cellkärnan och aktinet och skannade flera olika nivåer av cellen för att omfatta hela dennes volym. Med hjälp av bilanalys kunde mängden av YAP som tillhör kärnan och cytoplasman komponeras till ett ratio.

För att kunna jämföra kopplingen mellan YAP aktivering och aktinets struktur i diverse miljöer, placerades celler på olika koncentrationer av fibronektin, ett protein som finns i ECM. I ett ytterligare experiment, korslänkades fibronektinet på så sätt som gör att det blir svårare för cellen att hantera och bygga om det. Genom att ändra på cellens omgivning på detta sätt, varieras andelen integriner som kan binda sig. Således, påverkas hela mekaniska signalleringsprocessen. De tidigare beskrivna experimenten utfördes således på celler utsatta för växlande förhållanden.

Resultaten visar att aktinordningen blir mer organiserad vid ökad koncentration av fibronektin och blir mer slumpartad då matrisen är korslänkad. Detta kan bero på att vid låg tillgång till fibronektin, kan inte integriner binda sig lika bra till sin omgivning, som gör att det blir svårare för fokaladhesionerna att formas. I sin tur påverkar det aktinstrukturen. Det blir alltjämt svårare när ombyggnaden av matrisen är begränsad. Å andra sidan visade det sig att YAP aktiveringen förhåller sig på ett mer komplicerat sätt till omväxlingarna och korrelerar inte aktintrenden fullt ut. En förklaring till det kan vara att vi ser mekanisk reglering blandat med Hippo cellsignalering. Dock behövs det fler experiment för att dra några slutsatser.

Contents

4 Introduction

Cancer is a group of diseases that can arise in nearly any kind of tissue in almost any part of the body. According to estimates from the World Health Organization, cancer is the second most dominant cause of mortality worldwide, guilty of approximately 10 million deaths per year [1].The identifying characteristics are the formation of anomalous cells that can divide rapidly in an uncontrollable manner as well as invade other places of the body and form so-called metastases. The metastases are the primary cancer-associated cause of death. [1] That is why it is of vast importance to, in detail, investigate the processes involved in the formation and spreading of cancer.

Abnormal cell behavior, in diseases such as cancer, does not only depend on genetic mutations but also alterations in the tissue microenvironment[2]. These include changes in the extracellular matrix (ECM) composition and mechanical properties. This project focuses on the possible cross-talk between the regulation of YAP and F-actin organization in subcellular structures. YAP is responsible for cell proliferation and cell migration while F-actin is involved in cellular sensing of the microenvironment [2]. We examined the response of both components to see if they in any way correlate with each other. As YAP is highly involved in the cellular decision-making process, its appropriate functioning and activation are necessary to avoid disease provocation [2]. That is why it is important to gain an understanding of the activation processes of YAP.

This thesis is structured as follows:
First, I explain the relevant biological concepts, hereafter, the microscopy setup for the F-actin organization is described together with the model that allows for quantification of the organizational degree of F-actin. Later, I define the performed experiments and then present the detailed methods and results. Finally, I discuss the results.

5 Biological background

5.1 Mechanical forces in biology

Cells are constantly sensing the complex microenvironment that surrounds them. This environment is composed of the other adjoining cells, chemical compounds, interstitial fluids, and the ECM, which is a mixture of different molecules and proteins. Cells can distinguish biochemical signals, like hormones and cytokines, as well as recognize physical and mechanical properties of the microenvironment, for example, temperature, stiffness, elasticity, shear force, and pressure. Some mechanical cues, such as stiffness and shear force have a magnitude and a direction, others, such as concentration, can be presented in form of a gradient. [3][4]

5.2 Mechanotransduction

The process where cells sense and respond to mechanical forces is called mechanotransduction. During this process, cells can convert mechanical information from the microenvironment into biochemical signals. Mechanotransduction occurs in three different phases; sensing, transmission and response. Force can be relayed along with the cytoskeleton of the cell, which includes actin, microtubules, and intermediate filaments after the forces are sensed by the transmembrane proteins. The mechanosensitive proteins change their conformation and function upon force application, enabling the propagation of signals. That can in turn trigger downstream events which for example can influence transcriptional factors as the response of the cell. [5]

5.2.1 Cell migration

Many cells in multicellular organisms need to migrate, to enable proper organization and function. They can migrate either collectively in sheets or as individual cells. Some processes, for example, wound healing and embryonic development, require collective cell migration. Other processes, such as the migration of leukocytes to the infection sites can be categorized as single-cell migration. Deviated cell migration can instead be a mediator of pathologies such as cancer. If an individual cancer cell or a group leaves the primary tumor through the surround-

ing stroma and follows the bloodstream or lymphatic system it can form another colony elsewhere in the body. This process is called metastasization. [6]

5.2.2 Cell transcription

Mechanical cues from altered ECM properties can influence proteins residing in the cytoplasm and result in their structural modification and relocalization into the nucleus where they can activate transcription factors [7]. Studies show that the transcription process can be coordinated by condensation of various particles around the transcription complexes to which they can deliver necessary proteins. The transcription factors bind to DNA promoter elements and stimulate the synthesis of RNA by RNA polymerase enzymes. Transcription is an essential step in the gene expression process and consequently the determination of specific cell function. [8]

5.3 Focal adhesions

To examine the environment, cells assemble physical links that can attach them to the ECM. The adhesions can be made in different ways, including nonspecific electrostatic interactions and integrin, selectin, or cadherin-based specific binding. [6] Integrin based focal adhesions (FAs) have a central role in mechanosensing. [3] FAs are composed of multiple building blocks; the ECM proteins on the outside, transmembrane proteins, cytoskeletal proteins that provide a scaffold, and signaling proteins. When cells migrate, focal adhesions assemble and disassemble to relocate the cell by breaking up contacts and generating new. [6]

5.3.1 Integrins

Integrins are proteins that span the cell membrane to create a physical link between the FA adaptor proteins (such as talin which then binds to the cytoskeleton) and the ECM, making communication in both ways (outside in and inside out) possible. They are heterodimeric, which means they are composed of two distinct subunits α and β, existing in different variations. There are 18 types of registered α subunits and 8 types of β subunits which can be present in 24 combinations, each recognizing different ECM ligands and motifs. For example, $\alpha_v\beta_3$ integrins

can recognize RGD motifs that are present on ECM proteins, such as fibronectin and vitronectin. [9] Another integrin, $\alpha_5\beta_1$, requires an additional synergy site in proximity to the RGD motif for maximal binding. [10]

Integrins heterodimerize, forming pairs of subunits, in the endoplasmatic reticulum and Golgi apparatus and are transported to the plasma membrane where they can diffuse in their inactive form. The heterodimer activates upon force application from the ECM and its conformation changes as it unbends and the integrin legs separate allowing for increased ligand affinity. As the force proceeds, integrins start to form clusters and other proteins are recruited, which link to the actin cytoskeleton and the maturation of FAs occurs. When at the plasma membrane, integrins are continuously exposed to mechanical forces and serve as both the sensors and transmitters. The forces can consequently regulate the clustering into adhesion complexes, ligand binding kinetics, and the conformation of integrins themselves. [9]

It has as long been demonstrated that, in migrating fibroblasts, integrin-based FA complexes can sense directional mechanical cues by actively ordering the integrins concerning the direction of the force. Integrins polarize by coaligning with each other and orient themselves inside the FAs, tilting as a response to cytoskeletal forces acting upon them. [4]

5.3.2 F-actin

Filamentous actin (F-actin) is coupled to the integrins via adaptor proteins and is involved in the mechanotransduction process. F-actin constitutes a branched network of thin polymer filaments that can polymerize faster on the plus ends compared to the minus ends and can both add monomers in straight and branched configuration. By polymerizing towards the membrane it can protrude against the leading edge and generate a force onto the cell membrane, simultaneously experiencing backward force towards the center of the cell. This process also called ”retrograde flow”, can promote the maturation of FAs and increase the capability of mechanosensing. Another necessary mechanism is the non-muscle myosin II dependant contractility which generates pulling force on the actin cytoskeleton, which can be further transmitted to the ECM via integrins.[11] The complex

is called actomyosin. The actomyosin bundles are mainly regulated by Rho GT-Pases, which provides the modulation of the assembly dynamics and functions. [12]

Actin is the most abundant cytoskeletal protein in a cell. The fibers are flexible and thin, approximately 7 nm in diameter, while the length can reach up to several micrometers. The structure of F-actin is highly ordered and the network can form 3-dimensional bundles. [13]

5.3.3 Yes-associated protein 1 (YAP)

Yes-associated protein 1 (YAP) is a protein that is a transcriptional coregulator, involved in several biological processes, such as cell proliferation, survival, organ growth control, and cell differentiation. It is one of the main participants in the so-called, canonical Hippo signaling pathway, which controls organ size through the regulation of the above-mentioned cell functions. YAP can shift its location between the cell nucleus and the cytoplasm. In the cytoplasm, it is found in inactivated or degraded form. When YAP is in the nucleus it can interact with the family of DNA-binding factors (TEAD) which share a transcriptional enhancer factor (TEA) domain. This way transcriptional regulation can be achieved. [14]

Recent findings suggest that YAP plays an important role in mechanotransduction. [3] It has been discovered that YAP is involved in the cellular response to various mechanical cues such as the stiffness of ECM and restricted cell geometry. In cells restricted to a small area, YAP tends to shuttle into the cytoplasm as opposed to nuclear localization of YAP when cells are allowed to spread properly enabling F-actin contractility. Other situations that lead to nuclear YAP localization are the high stiffness of ECM and ECM remodeling. This property of YAP is crucial for the translation of the information from mechanical cues, to produce the appropriate cell behavior and gene expression. [3]

Several suggested mechanisms potentially regulate YAP activation. The primary source of YAP activation seems to be the contractility of myosin and F-actin cytoskeleton and actin remodeling, where RHO kinase may play a certain role. Still, it is unclear how this information can be translated into signaling. Another the-

ory is that the composition of FAs regulates YAP as FA components get recruited differently depending on the forces they sense. [3][12] The cytoskeleton may also be able to apply forces onto the cell nucleus, stimulating the nuclear pore complex and allowing the transport of macromolecules into the nucleus. [12]

5.4 Other relevant topics

5.4.1 Fibroblasts

During this project, the focus was put on single-cell migration of fibroblasts, whose main task is to synthesize various glycoproteins of the extracellular matrix (ECM), including fibronectin and collagen. Fibroblasts can migrate into wounds and proliferate after receiving various biochemical and mechanical ECM cues enabling wound healing and tissue repair. [6]

5.4.2 Fibronectin

Fibronectin (FN) is an ECM protein critical for cell adhesion, growth, and directed tissue organization. It can be divided into plasma FN and cellular FN. Plasma FN is expressed by hepatocytes and secreted into blood plasma to circulate, while cellular FN is synthesized by fibroblasts together with other cell types and deposited into surrounding ECM. Secreted FN is inactive and composed of soluble dimers that can be remodeled into insoluble fibers through a force-generating integrin-mediated cell binding.[15].

FN contains an RGD binding site that is recognized by integrins $\alpha_v\beta_3$ and $\alpha_5\beta_1$ ($\alpha_5\beta_1$ can additionally bind to a so-called synergy site) and it has been shown that FN coating stimulates directional persistence and polarization of fibroblasts. It is possible, that cells can be guided while remodeling and unfolding the surrounding FN fibers and thus decide the direction of migration [15].

5.4.3 Cross-linked Fibronectin

FN coating can be cross-linked using glutaraldehyde to generate inter-and intramolecular links, connecting FN fibers to the glass surface [15]. We hypothesize,

that by cross-linking the matrix, the access of $\alpha_5\beta_1$ integrins to both the RGD motif and the synergy site can be restricted to some degree and the FAs are maintained predominantly by $\alpha_v\beta_3$ integrins.

5.4.4 PLL-control

Poly-L-lysine (PLL) was used as the negative control because it allows for a non-specific binding that does not require integrins, unlike FN or type I collagen [16]. The attachment instead depends on the electrostatic interaction between polyanionic cell surfaces and polycationic PLL [17].

5.4.5 Paxillin

Paxillin is an adaptor protein that is a major component in FAs. Paxillin arrives at the cell leading edge when the FAs are forming and stays there until the upcoming FA disassembly is completed. The main role of paxillin is to recruit the necessary molecules that are involved in cell migration by providing docking sites enabling mature FA assembly. [18]

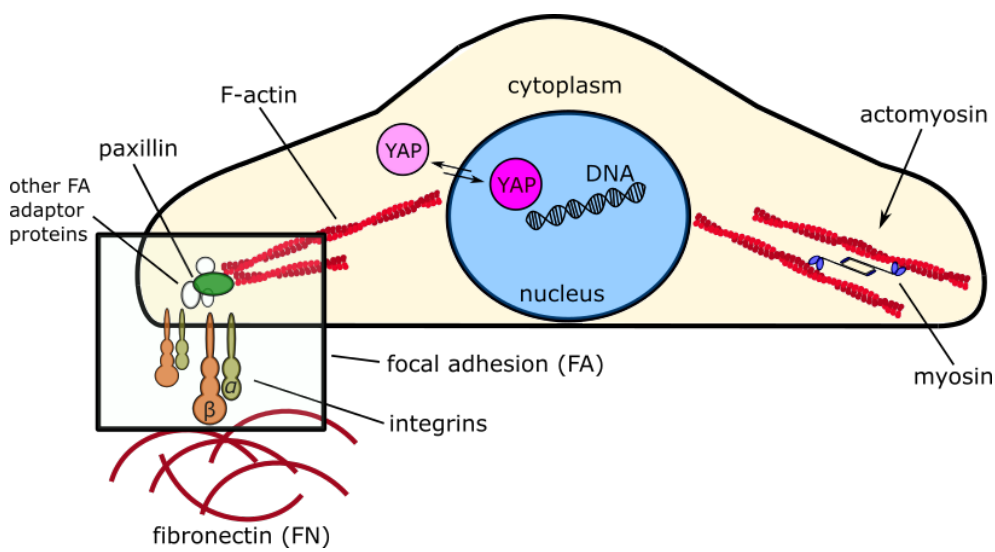

Figure 1: **Sketched cross-section of a fibroblast.**

6 Scientific question

The goal of this project is to extend the knowledge of the mechanotransduction pathway and its regulation of YAP. The measured properties are YAP activation, FA and cell morphology together with F-actin architecture in FAs as a response to varying degrees of integrin activation. Integrin activation is altered through modifications of the ECM, by providing different accessibility to FN ligands.

7 Polarization and fluorescence anisotropy in bioimaging

7.1 TIRF

In a 2D experiment, FAs form at the interface between the cell and the ECM coated surface that the cells are plated on and can attach to. To achieve proper imaging of these structures and increase the signal-to-noise ratio one needs to restrict the excitation to a very thin volume layer just above the interface. [19] For this reason a Total Internal Reflection Fluorescence (TIRF) microscope is preferable.

In the TIRF setup, the sample is illuminated with an excitation laser beam that is incident at an angle above "critical angle" ($\theta > \theta_c$) with respect to the normal arising from the glass surface, see Snell's law:

$$\theta_c = sin^{-1}(\frac{n1}{n2})$$

where $n1$ is the refractive index of the sample that is composed of cells immersed in a liquid and $n2$ of the solid slide that the sample is mounted upon. [19]

In this case, the light gets totally reflected from the interface and continues back into the solid, instead of being transmitted with the refraction angle if the condition is $\theta > \theta_c$. As a consequence, a part of the incident energy continues through the interface into the sample and propagates parallel with respect to the surface. This field is called the evanescent wave and it decays exponentially further away from the surface.

$$I(z) = I_0 e^{-z/d)}, d = \frac{\lambda}{4\pi}(n_2^2 sin^2\theta - n_1^2)^{-1/2}$$

where I is the intensity and z is the distance from the surface. Depth d is dependant on λ_0 which is the wavelength of the excitation light in vacuum and is independent of light polarization. This way d is decreasing with increased θ, implying a thinner volume of excitation. [19] Usually the depth of the excited volume is around 50-150 nm depending on the NA of the objective (typically 125 nm for a 1.45 NA). That way the background fluorescent is reduced and the signal to noise ratio is increased.[20]

I_0 is dependent on polarization and θ. The excitation light originated from a laser can be either s or p polarized. P-polarized light has an electric field oriented parallel to the plane of incidence, whether s-polarized is perpendicular. The setup used in this experiment has an s-polarized laser source. In this case, the evanescent wave is also plane-polarized, perpendicular to the plane of incidence, and has an I_0 that is [19]:

$$I_0 = \frac{4cos^2\theta}{1 - (n_1/n_2)^2}$$

In the case of p-polarized excitation, the evanescent wave gains components of other spatial orientations which make the expression more complex and makes the polarization of the field elliptical. [20] The TIRF microscopy setup, per se, does not require polarization, but this particular project benefits from that additional ability.

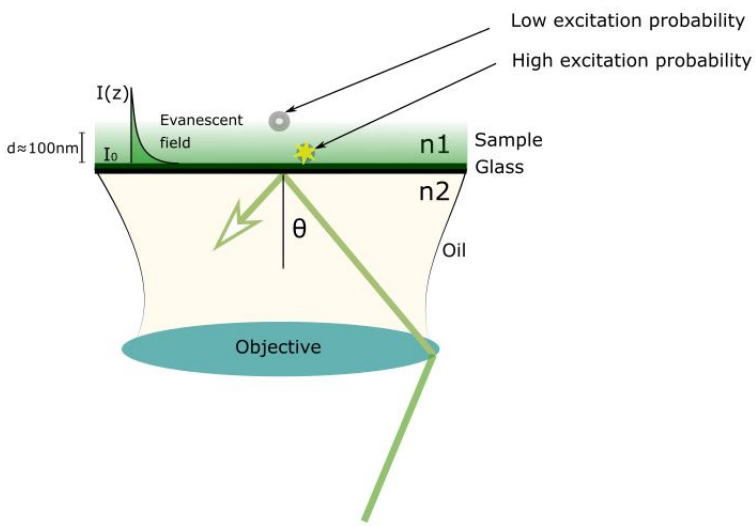

Figure 2: **TIRF schematics**.

7.2 Fluorescence anisotropy

Polarized excitation of a fluorescent anisotropic sample gives rise to polarized emission. It is caused by absorption and emission transition moments of fluorophores that are structure dependant and oriented along with specific directions. A fluorophore that has its transition moment oriented parallel with respect to polarized light will therefore be excited, unlike a fluorophore with a transition moment oriented perpendicularly. In a homogenous solution, the stochastic orientation of fluorophores will give rise to selective excitation.

Placing a polarizing beam splitter (PB) in the emission path allows for the separation of light with parallel and perpendicular polarizations. Observed intensities in the two channels, after being separated, are designated as $I_{\parallel}$ and $I_{\perp}$ respectively. Fluorescence anisotropy can be calculated using the following relationship:

$$r = \frac{I_{\parallel} - I_{\perp}}{I_{\parallel} + 2I_{\perp}}$$

where the numerator is the difference between the two channel intensities and the denominator stands for normalization, total intensity. Anisotropy is dimensionless and in the ideal case independent of the amount of fluorescence or intensity. [21]

There are causes for fluorescence depolarization. The main cause is the displacement between the absorption and the emission moments. One factor is the effect of resonance energy transfer (RET) which can occur among fluorophores in solutions with high concentration. RET takes place when one excited fluorophore (donor) transfers the energy to another fluorophore in proximity (acceptor). RET can be radiative and non-radiative. Another factor is rotational diffusion that can affect the orientation of the fluorophores transition moment during its lifetime while being in the excited state. That depends on the viscosity of the media where the fluorophores are located and the size and shape of the fluorophore itself. [21]. The rotational diffusion measurement can be found in the Annex, Figure 14.

Optical components in the emission pathway, for example, dichroics, usually exhibit differences in transmittances for the light of different polarizations. This can lead to biased results and errors in quantitative analysis. To account for that a cor-

rection factor, also called G-factor, can be calculated and introduced in the formula for fluorescence anisotropy. In a TIRF setup, the G-factor image is acquired by imaging a dilute concentration of a small fluorescent dye, for example, fluorescein (isotropic sample), using the same camera settings as for normal TIRF imaging, but instead a mercury lamp as an excitation source to avoid the polarization effect from the laser. The definition for G-factor is [20]:

$$G_{factor} = I_{\parallel}/I_{\perp}$$

where $I_{\parallel}$ and $I_{\perp}$ are the intensities of the parallel and the perpendicular channels respectively.
The G-factor corrected fluorescence anisotropy formula is [20]:

$$r = \frac{I_{\parallel} - G_{factor} I_{\perp}}{I_{\parallel} + 2G_{factor} I_{\perp}}$$

A drawback of using a high numerical aperture is that it causes mixing of polarization. As the light is collected at a large angle, an orthogonal component disrupts the signals in the $I_{\parallel}$ and $I_{\perp}$ channels. One can correct for that effect theoretically, by calculating Axelrod's correction factor. Although, it assumes that the sample contains isotropically oriented fluorophores.[22] That is not the case in this particular experiment, thus the correction was not used.

7.3 Fluorescence anisotropy of filamentous structures

Fluorescence anisotropy is an effective tool in biomedical research. It can reveal the size, mobility, and rotational diffusion of molecules, as well as evaluate interactions and distances between molecules with Förster resonance energy transfer (FRET).[22] Additionally, it enables measurements of structural organization in an ensemble of filaments besides the pure detection and spatial localization. That can lead to a deeper understanding of the biological function. Importantly, one has to remember that the optical diffraction limit restricts the spatial resolution and consequently the registered signal is an average of several filaments in the structure (the diameter of an actin filament is approximately 7nm and the spatial resolution for a conventional TIRF setup is 0.2μm). Also, as the signal emerges from the attached fluorophores and not directly from the filaments themselves, the information is a composition of the filament orientation and the rotational mobility of the fluorescent probe, which depends on the properties of the linker that couples them together. [23]

For this experiment, Alexa Fluor 488-phalloidin was used for actin labeling. Because of the specific molecular structure the dipole of this dye points along the direction of the fiber that it attaches to. It is coupled with a linker that restricts its position and rotation but allows for wobbling to some extent. The maximum wobbling aperture of a single molecule, δ, is 90°. [23]. An additional experiment, where a different dye, SiR, was used for f-actin labeling, can be found in the Annex, Figure 15. SiR dipoles are oriented perpendicularly with respect to the f-actin filament orientation.

The model, that allows the performance of anisotropy measurements in FAs is described in Figure 3. It relies on the properties of FAs themselves, namely their elliptical form, which has a long axis, often pointing perpendicularly with respect to the leading edge of the cell. By calculating the mean anisotropy value of each FA in an image and extracting the respective FA long axis orientations, one can gather the information in a plot: mean anisotropy of F-actin in FA as a function of FA long-axis orientation. The anisotropy values will vary, depending on the intensities in the $I_{\parallel}$ and $I_{\perp}$ channels. After collecting an adequate number of data points, belonging to the same condition (not necessary from a single image) a

trigonometric function (7.3) can be fitted, that describes the trend. [4]

$$f(x) = A \cdot cos^2(x + \theta) + C$$

where x are the data-points (mean anisotropy of F-actin in FA as a function of FA long axis orientation) and [4]:

- Amplitude (A) describes the fraction of coaligned fluorophores in the ensemble. High A implies high anisotropy and consequently a high fraction of coaligned fluorophores.
- Phase shift (θ) defines the average orientation of dipoles in the ensemble of fluorophores. If the phase shift is at 0°, the average orientation of dipoles is aligned with the orientation of polarized excitation. That means that the dipoles are oriented along the FA long axis.
- Offset (C) is not completely understood. However, it does not contribute to the information about the alignment of fluorophores.

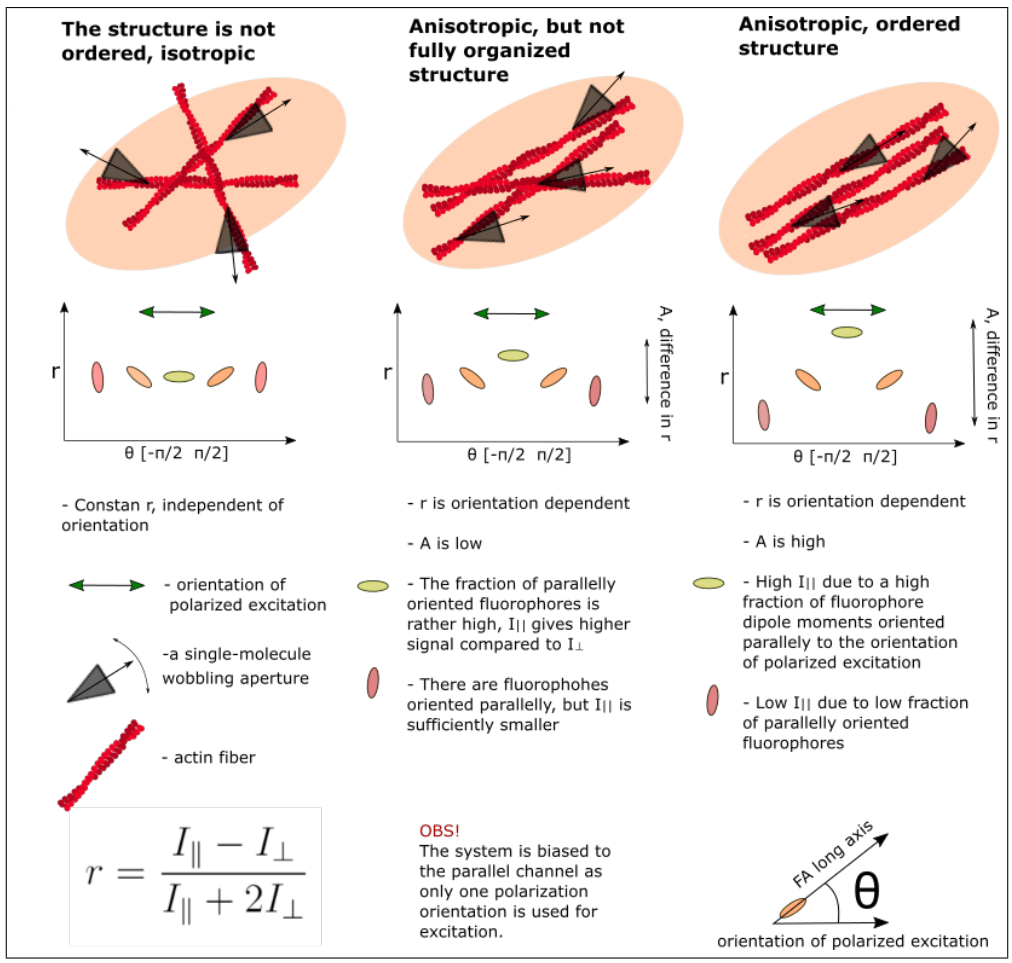

Figure 3: **Model, describing anisotropy measurements in FAs**

8 Methods

8.1 Experiments

Mouse embryonic fibroblasts (MEFs) cell line was used for the experiments. The cells were cultured in Dulbecco's high glucose modified eagle medium (DMEM + glutaMAX, Gibco, 61965026), 10% fetal bovine serum (Gibco,10270106) and Penicillin/Streptomycin (Gibco, 15140122). Cells were incubated at 37°, 5%CO2.

Two experiments were designed:

- **Alteration of FN concentration**
  The concentration of FN was varied according to Table 1 to generate different amounts of accessible ligands for integrins $\alpha_v\beta 3$ and $\alpha_5\beta_1$ to attach to. The readout from all conditions was the F-actin anisotropy and YAP localization. PLL coating was used as a control, as it promotes nonspecific binding.

- **Restriction of ECM remodeling and ligand accessibility**
  The FN coating was cross-linked (also abbreviated as cl) at two chosen concentrations, 0.1μg/ml FN and 10μg/ml FN (see Table 1) to restrict the remodeling of ECM as well as to provide lower ligand accessibility. The hypothesis is that integrin $\alpha_5\beta_1$ will not be able to bind as easily to the cl FN because the chance of binding to both the RGD motif and the synergy site is less feasible.

0.1ug/ml FN	1ug/ml FN	10ug/ml FN	50ug/ml FN	PLL
0.1ug/ml FN cl.		10ug/ml FN cl.		

Table 1: Experimental conditions: different FN concentrations together with the PLL control and the cross-linked conditions.

In all experiments, MEFs were fixed after 4 hours of incubation on the appropriate coating. The reason was to bypass FN produced by the fibroblasts themselves and consequently ensure the outlined conditions.

For samples that were not cross-linked, the glass bottom dishes were immersed in the respective concentration of FN in Phosphate buffered saline (PBS, Gibco) and incubated at 37° for 30 min. Thereafter, they were blocked with 2% Bovine Serum Albumin (BSA, Sigma Aldrich) in PBS for 45 min at 37°.

The preparation of the cross-linked samples included an extra step before the blocking. The FN solution was aspirated and the samples were washed once in PBS before adding 1% Glutaraldehyde solution (25% in H_2O, Sigma Aldrich) in PBS and incubated for 15 min at RT. Thereafter the sample was washed three times with PBS.

8.2 F-actin anisotropy

This experiment was designed to determine F-actin organization/anisotropy in FAs. Cells were plated on glass-bottom dishes coated with FN and fixed after 4 hours. F-actin was labeled using phalloidin conjugated to Alexa488, which are sufficiently rotationally constrained and have a dipole moment oriented parallel with respect to actin filaments. Additionally, paxillin was immunostained with primary mouse anti-paxillin antibody and goat anti-mouse Alexa 568 to get an indication of FA localization. The TIRF setup equipped with an Optoplit with inserted R/G cube and a polarization beamsplitter (PBS) was used for imaging. The image analysis and data extractions were performed in MATLAB [24]. The results were compared across the previously described conditions.

8.2.1 Sample preparation

Firstly, 35 mm 1.5 glass-bottom dishes (Cellvis, D35-20-1.5-N) were coated according to previously mentioned conditions and blocked with 2% Bovine Serum Albumin (BSA, Sigma-Aldrich) for 40 min at 37° (if cl, see 8.1). MEFs were plated for 4 hours and thereafter fixed with 4% paraformaldehyde (16% Formaldehyde (w/v), Methanol-free, Thermo Scientific) in cytoskeletal buffer (CB) for 20 min at 37° and permeabilized with 0.5% Triton TX-100 (Sigma-Aldrich) in CB for 5 min at RT. Afterward, the sample was washed with 0.1M glycine in CB for 10 min, gently rocking, and washed with Tris Buffered Saline buffer (TBS), also gently rocking, once for 5 min and twice for 10 min. Next, the sample was blocked with 2% BSA in TBS for one hour and immunostained with primary mouse anti-paxillin IgG1 antibody (BD Transduction Laboratories) (1:500) diluted in 2% BSA in TBS overnight at 4°. Thereafter, the sample was washed three times with Tris-Buffered Saline, 0.1% Tween (TBST), 5 min each, while gently rocking, before adding the secondary goat anti-mouse IgG Alexa 568 (Invitrogen) (1:400) and Alexa Fluor 488 Phalloidin (Invitrogen) (1:500) diluted in 2% BSA in TBS, incubating in a dark environment at RT for two hours. Lastly, the sample was washed three times with TBST, 5 min each, while gently rocking. Finalized samples were immersed in TBS and were kept in the fridge at 4°.

8.2.2 Imaging

Samples were imaged using the EA-TIRFM setup (Nikon TIRF microscope coupled to OptoSplit III (Cairn Research)), equipped with a 100X objective (NA = 1.49) and Photometrics Prime 95B sCMOS camera (11 μm x 11 μm Pixel Area). The emission path was split into three channels with an OptoSplit supplied with a red/green (R/G) dichroic cube and a PB leading the emitted light into three separate channels on the camera field. This setup enabled the simultaneous recording of parallel and perpendicular polarized emission of the "green" spectra originated from the phalloidin 488 dye and "red" spectra from the Alexa Fluor 568 dye. The drawback was the restricted imaging field. The schematics of the optical pathway are illustrated in Figure 4.

Starting every imaging experiment, channels were manually spatially aligned by adjusting the OptoSplit. The laser power of both lasers and the exposure time was kept constant at all time to avoid possible bias. Cells were imaged using an appropriate TIRF angle. Background images (ten for each sample) of spots in the samples lacking cells were taken to account for background fluorescence.

For the G-factor measurements, an image was taken of a sample containing low FITC concentration (in water) while using a 488 diode for excitation and the same optical path as for the main experiment. Another image was taken of water for background correction. This procedure was done in conjunction with every imaging session.

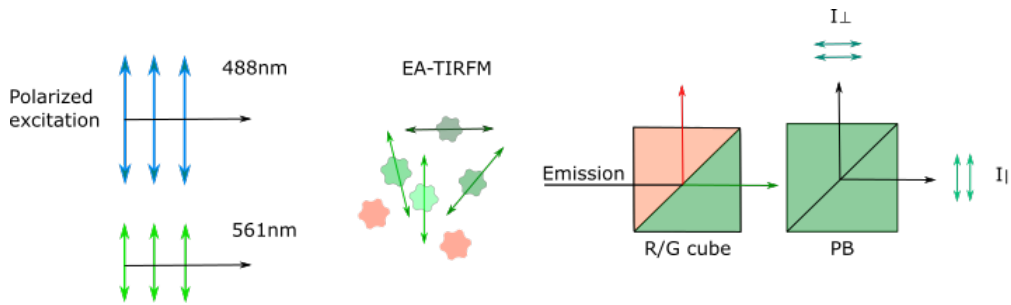

Figure 4: **Optical pathway**. Plane polarized 488 nm light (marked as blue arrows) is used for excitation of F-actin - Phalloidin 488 (green molecules) in TIRF mode. Depending on the fraction of coaligned dipoles with respect to the orientation of polarized excitation the fluorophores will emit red-shifted light (520 nm), carrying additional information about the dipole orientation. Simultaneously, a 561 laser is used for excitation of paxillin - Alexa 568 (marked as light green arrows). Before the emitted light of respective wavelengths reaches the camera, it passes through an R/G filter cube and a PB. The R/G cube reflects the wavelengths of the red-shifted spectra and transmits the green-shifted wavelengths. The PB reflects the perpendicularly polarized light and transmits the parallel polarized light. As the redshifted light is filtered out before reaching the PB, only the light emitted by Phalloidin 488 is split. This way the camera screen contains three channels: signal originated from paxillin - Alexa 568 (FA marker), together with parallel and perpendicular channels containing the F-actin - Phalloidin 488 emitted light.

8.2.3 Image analysis

- **Cropping**
  Images were slightly cropped to exclude the possible overlap from other channels and empty areas. An example of the three output channels can be seen in Figure 5a).

- **Alignment**
  Images were aligned using the property of the F-actin network to exhibit similar intensity patterns in the parallel and the perpendicular channels. A

MATLAB inbuilt function "imregtform" was applied to estimate a geometric transformation based on intensities in the images to optimize the spatial alignment pixel-wise.

- **G-factor correction**
  An image of low FITC concentration was background corrected by subtracting the water sample image from the respective channel ($I_{\perp}$ and $I_{\parallel}$). A new matrix/image was generated by pixel-wise division of the images from the parallel and the perpendicular channel ($G_{factor} = \frac{I_{\perp}}{I_{\parallel}}$).

- **Background correction**
  A mean value pixel-wise matrix was calculated given the ten background images to correct for background fluorescence. Median filtering was performed to eliminate the "salt pepper" effect.

- **Anisotropy map**
  Anisotropy maps were calculated for every cell image by applying the fluorescence emission anisotropy formula to the background subtracted parallel and perpendicular images pixel-wise ($r = \frac{I_{\parallel} - G_{factor} \cdot I_{\perp}}{I_{\parallel} + 2 \cdot G_{factor} \cdot I_{\perp}}$). An example image of the anisotropy heat map is shown in Figure 5b).

- **Focal adhesion binary mask**
  FAs were segmented in the Alexa Fluor 568 paxillin channel by applying different filtering operations in a specific sequence: firstly, Gaussian smoothing with a small standard deviation to denoise the image, secondly, maximum filtering to dilate the intensity peaks. The threshold level was determined by combining the Otsu-threshold with the Rosin-threshold level. Based on the threshold level a binary mask could be created. An FA binary mask example is presented in Figure 5b).

- **Extraction of FA properties**
  The binary mask was multiplied with the anisotropy map to segment focal adhesions. The FA-related properties could be extracted using the MATLAB inbuilt function "regionprops". The extracted measures were: the orientation of the FA long axis with respect to the x-axis, a list of all pixel-anisotropies

in a FA, FA area, and eccentricity. The principle of extraction of the FA long axis orientation with respect to the x-axis is demonstrated in Figure 5c).

- **Anisotropy plot**
  All image data belonging to the same physical sample was gathered into one plot where a mean anisotropy value was established per FA and plotted versus the FA long-axis orientation. A trigonometric function ($f(x) = A \cdot cos^2(x+\theta)+C$) was fitted to the data points using MATLAB's "curve fitting tool" application to represent the data as amplitude (A), phase (θ) and offset (C). The goodness of fit could also be extracted.

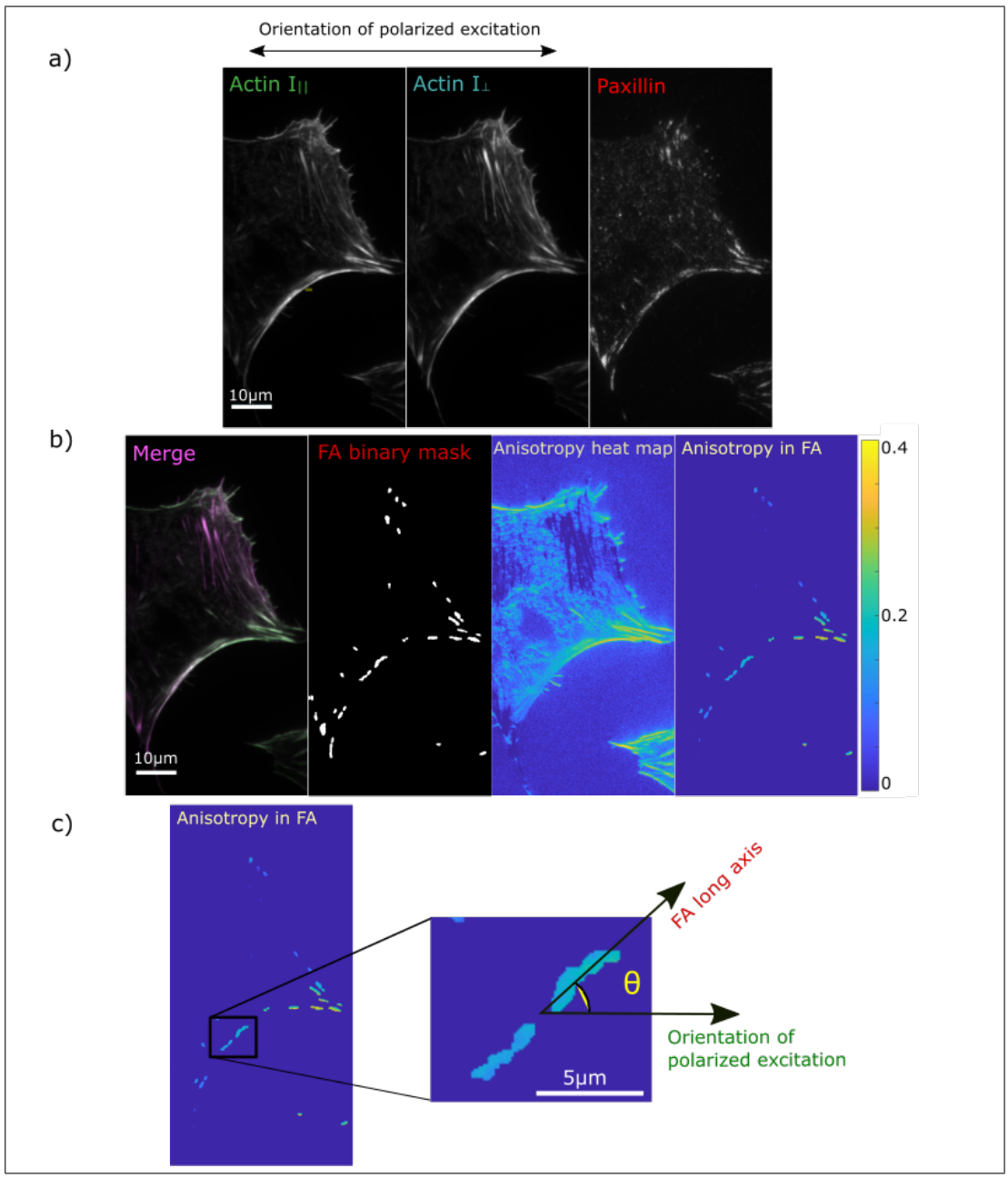
a)
Orientation of polarized excitation
Actin I||
Actin I⊥
Paxillin
10µm
b)
Merge
FA binary mask
Anisotropy heat map
Anisotropy in FA
0.4
0.2
0
10µm
c)
Anisotropy in FA
FA long axis
θ
Orientation of
polarized excitation
5µm

Figure 5:

Figure 5: **a) Fluorescent images, demonstrating the output channels, imaged using the EA-TIRFM setup**. Fluorescence images of the three output channels: parallel and perpendicular channels originated from the emission of F-actin - Phalloidin 488 and paxillin - Alexa Fluor 568. The orientation of polarized excitation is shown. **b) Image analysis, extraction of F-actin anisotropy in FAs**. The first image (to the left): a merge of the two actin channels ($I_{||}$ and $I_{\perp}$). Second image: binary mask based on the Alexa 568 paxillin image. Third image: The anisotropy heat map is executed by applying the anisotropy formula with the appropriate G-factor to the two channels. To the right: a binary mask is applied on the anisotropy heat map to only segment information coupled to FAs. **c) Extraction of FA orientation**. A zoom-in of the FA anisotropy image: θ is the angle between the orientation of polarization excitation and the orientation of the FA long axis.

8.3 YAP activation

One way of measuring the degree of YAP activation in a cell is to determine the nuclear/cytoplasmic ratio of YAP. [25] Increased nuclear localization of YAP implies more activation as the transcriptional regulation can be achieved. A relative measure is to prefer when comparing across different conditions. Cells were plated on glass-bottom dishes coated with FN accordingly. The MEF samples were fixed after 4 hours similar to the anisotropy experiment. For this experiment fibroblasts were immunostained with primary mouse-anti YAP antibody and secondary anti-mouse 2° Alexa 568-conjugated antibody. To get an indication of the nuclear boundary the nucleus was stained with nuclear dye Hoechst 350 and F-actin was stained with Phalloidin Alexa Fluor 568 for the cytoplasmic termination. A confocal microscope was used for imaging of the samples and Z-stacks were taken to capture the whole cell volume. The image analysis procedure was executed in MATLAB.

8.3.1 Sample preparation (YAP):

MEFs were plated on glass-bottom dishes coated accordingly to previously described ECM conditions and fixed with 4% paraformaldehyde in PBS, for 30 min in room temperature, after 4 hours of incubation. Next, cells were permeabilized with 0.2 % Triton TX-100 in PBS for 5 min at room temperature and after, blocked with 3% BSA in PBS for 45 min at room temperature. Cells were immunostained with primary mouse-anti YAP monoclonal IgG_{2a} antibody (Santa Cruz biotechnology) (1:100) in 1% BSA, PBS and left at 4° overnight. The next day, cells were washed 3 times for 1 min with 0.05% Tween (Sigma-Aldrich), PBS. Thereafter, the samples were incubated for two hours in secondary goat anti-mouse 2° Alexa 568-conjugated IgG antibody (Life Technologies Corporation) (1:400), nuclear dye Hoechst 350 (33342 Solution, Thermo Scientific) (1:4000), and Alexa Fluor 488 Phalloidin (Invitrogen) (1:500) in 1% BSA, PBS. After incubation cells were washed 3 times for 1 min with 0.05% Tween, PBS, and rinsed with PBS.

Complete samples were mounted using ProLong Glass Antifade Mountant (Invitrogen) and lidded with a coverslip. The samples were left to dry properly overnight and could later be stored at 4°.

8.3.2 Imaging

Samples were imaged using a Nikon Confocal A1RHD microscope (Detectors: 2 GaAsP PMT (for 488 and 561 lines), 2 PMT (for 405 and 640 lines), and 1 GaAsP PMT (spectral detection)) equipped with three excitation lasers to each match the fluorescent profile of respective fluorophore present in the sample (laser line 405 nm - Hoechst (nucleus), 488 nm - Phalloidin 488 (F-actin), 561 nm - Alexa Fluor 568 (YAP)). The laser intensities, once chosen, were kept constant for the rest of the imaging procedure to avoid possible bias. Z-stacks were taken with a step size of 0.6 μm in an optimized range, using a 100X objective, to capture the whole cell volume. An equivalent Z-stack was taken of the background in connection with every sample.

8.3.3 Image analysis

Identical image analysis procedure was applied to all images:

- **Pretreatment and background subtraction**
  All images were reformatted from ".nd2" to ".tiff" and saved as 16-bit grayscale files. The Z-stack layer images for each channel (nucleus, f-actin, and YAP) were added up to form three respective images. The same procedure was applied to the background Z-stack, after which the background image was subtracted from the respective cell image channel to correct for the background fluorescence. Example images of all three channels (separate) and the merge are shown in Figure 6a).

- **Binary mask for nuclear YAP**
  The cell nucleus was segmented in the nucleus channel, using Otsu thresholding to derive the binary mask. Morphological closing was performed to remove eventual wholes (dark areas) in the object. This mask was responsible for the segmentation of nuclear YAP, an example is shown in Figure 6b).

- **Transition zone**
  The nuclear mask was dilated using a 10-pixel disk-shaped form, to create a transition zone neither belonging to the nuclear or the cytoplasmic segment.

- **Binary mask for cytoplasmic YAP**
  The last-mentioned dilated nucleus binary mask was once again dilated using a 30-pixel disk-shaped form, which the original mask was subtracted from. This resulted in a new doughnut-shaped binary mask, that selects the cytoplasmic YAP. In some images, this mask partly appeared outside the cell contour. Thus, to avoid it, the YAP signal was segmented in the F-actin channel, using the mean intensity value of all pixels as a threshold. The intersect of the doughnut-shaped mask and the F-actin mask resulted in a new optimized mask, that was used for segmentation of cytoplasmic YAP, a example is shown in Figure 6 (b).(***Note***: the F-actin binary mask itself was not used because the cell shape tends to get thinner further out from the center. The diminished amounts of YAP in the distal cell parts could affect the measurements.)

- **Measurements**
  Two previously described segmentations were applied to the respective YAP grayscale image and the mean intensity values in each segment could be calculated using the MATLAB inbuilt function ”regionprops”. The nuclear/cytoplasmic YAP ratio was estimated by dividing the mean intensity of the nuclear YAP by the mean intensity of the cytoplasmic YAP.

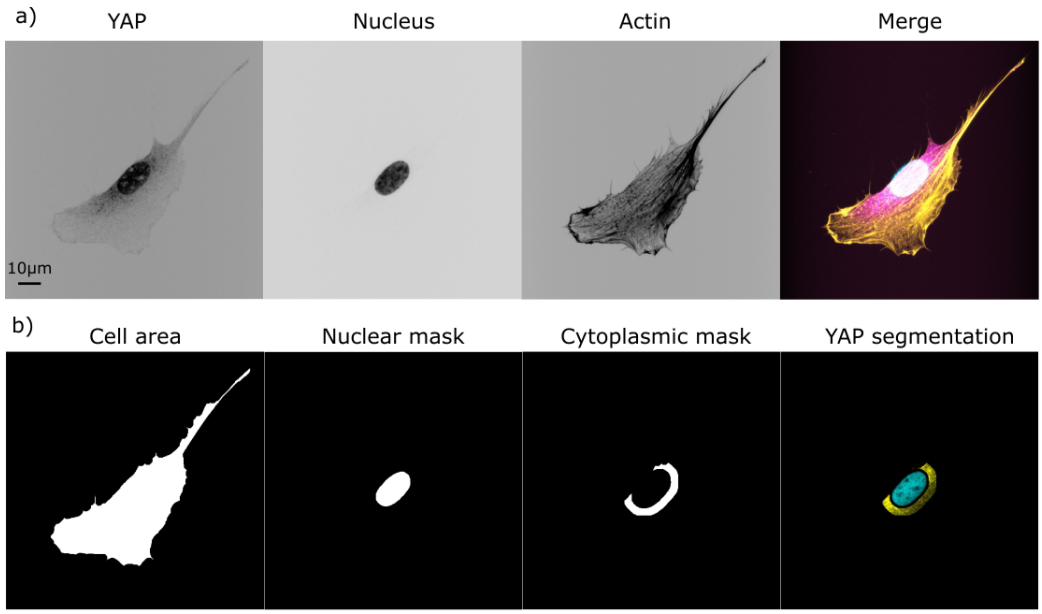

Figure 6: **Image analysis, nuclear and cytoplasmic YAP segmentation**. **a)** MEF cell plated on 1ug FN. From left to right: YAP signal, the nucleus, the F-actin, and the last image is a merge of all bio-markers (YAP - magenta, nucleus - cyan, and actin - yellow). **b)** The first image (to the left) shows an example of the cell area binary mask, executed by thresholding the F-actin signal. The second image illustrates the binary mask of the cell nucleus, which is used for the segmentation of the nuclear YAP. The next image shows the binary mask of the cytoplasmic YAP, which is an intersection of the dilated doughnut shape around the nucleus and the F-actin binary mask. The last image shows the nuclear and the cytoplasmic YAP. The transition zone is the empty area, that separates the two segments.

8.4 Cell area measurement

Cell area is an important property, which is expected to vary across the different conditions and is a decent indicator of the cell's well-being. In conditions that favor cell attachment, fibroblasts increase in the cell area. For cell area measurements the already prepared samples from both earlier experiments (anisotropy and YAP localization) were imaged with a low magnification objective (20X). Actin Phalloidin 488 was excited using solid-state lighting (Lumencor's SPECTRA X) of an appropriate wavelength (488nm) in EPI fluorescent mode.

Cells were segmented using the following algorithm:
To correct for uneven background illumination and autofluorescence a background image was extracted through a morphological opening with a larger structuring element, that removed the foreground objects. This background image was subtracted from the current image. Median filtering and a MATLAB inbuilt function "imadjust" was applied on the resulting image, to increase the contrast. Global Otsu thresholding was used for the image binarization and the border segments were removed by applying the "imclearborder" function. Segments below a certain size were removed, to exclude questionable objects. An example segmentation is shown in Figure 7. Cell area and cell eccentricity could be extracted from the segmentation, by using a built-in MATLAB function "regionprops".

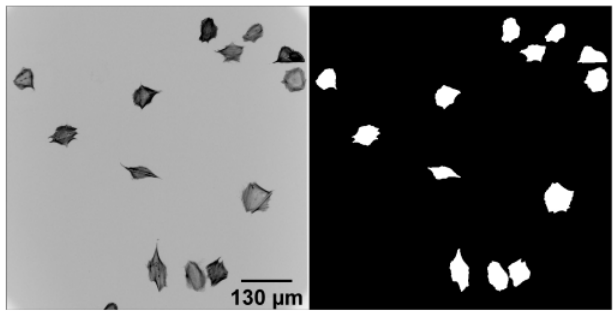

Figure 7: Cell area measurement, segmentation example. To the left is the original fluorescent image of the F-actin Phalloidin staining (MEFs plated on 10 μg FN) and to the right is the result of the segmentation achieved by the previously described procedure.

9 Results

9.1 Integrin activation regulates the cell and FA morphology in fibroblasts

We expected to see a change in both cell and FA morphology due to altered integrin activation. What we observe, based on the performed measurements, indicates, in fact, a strong correlation between the above mentioned parameters. Here, the morphological responses of fibroblasts to changes in ECM (FN) concentration are presented, see Figure 8. The measured morphological properties are cell area, cell eccentricity, FA area, and FA eccentricity.

The cell area and eccentricity measurements on the different conditions were extracted from the F-actin segmentation. The example fluorescent images are presented in Figure 8a). The clear trend is the linearly increasing cell area due to raised FN concentration in a given range, with cells having the smallest area when plated on FN=0.1μg and largest on FN=50μg Figure 8b). Interestingly, opposed to expectations, cells plated on the PLL result in a slightly larger cell area compared to FN=0.1μg. The cell eccentricity does not significantly change between the FN concentrations, but drops on the PLL condition 8c).

The focal adhesion area and eccentricity data were extracted from the Paxillin (FA marker) segmentation, the example images demonstrating FAs are presented in Figure 8d). The FAs are not pronounced on the control condition, therefore, the morphological FA properties could not be measured. The FA area increases on higher FN concentration, but does not change after FN=10μg, see Figure 8e). The FA eccentricity plot, in Figure 8f), is showing that the FAs, in addition to increased area, also become more elongated due to raised FN concentration.

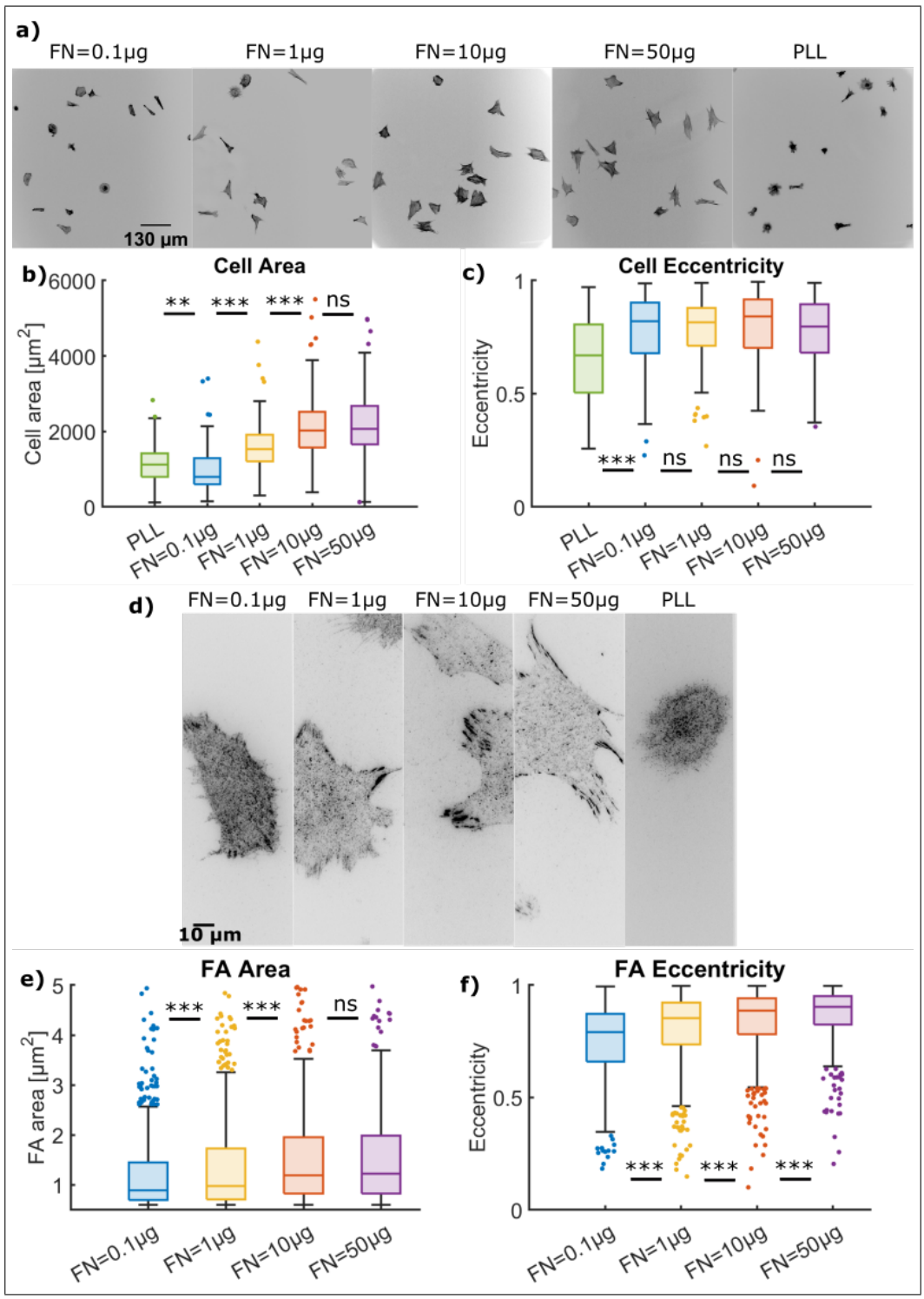
a)
FN=0.1µg
FN=1µg
FN=10µg
FN=50µg
PLL
130 µm
b)
Cell Area
Cell area [µm²]
6000
4000
2000
0
**
***
***
ns
PLL
FN=0.1µg
FN=1µg
FN=10µg
FN=50µg
c)
Cell Eccentricity
Eccentricity
1
0.5
0
***
ns
ns
ns
PLL
FN=0.1µg
FN=1µg
FN=10µg
FN=50µg
d)
FN=0.1µg
FN=1µg
FN=10µg
FN=50µg
PLL
10 µm
e)
FA Area
FA area [µm²]
5
4
3
2
1
***
***
ns
FN=0.1µg
FN=1µg
FN=10µg
FN=50µg
f)
FA Eccentricity
Eccentricity
1
0.5
0
***
***
***
FN=0.1µg
FN=1µg
FN=10µg
FN=50µg

Figure 8:

Figure 8: **Integrin activation regulates the cell and FA morphology in fibroblasts**. **a)** Fluorescent images (F-actin) of multiple single cells, taken in the EPI mode (20X objective), indicating the cell morphology associated with different FN concentrations (scale: 1.834pixels/μm). **b)** Cell area as a function of FN concentration. Each box-plot corresponds to cell areas (in μm^2) of 102 cells from 2 experiments. The extraction of the property is described in section 8.4. The median, the lower and upper quartiles together with outliers are shown in the plot. The p-values were calculated using a Mann-Whitney U-test: $P < 0.0037$ between PLL and FN=0.1μg, $P < 3 \cdot 10^{-15}$ between FN=0.1μg and FN=1μg, $P < 4 \cdot 10^{-5}$ between FN=1μg and FN=10μg, $P < .35$ (not significant) between FN=10μg and FN=50μg. **c)** Cell eccentricity as a function of FN concentration. Each box-plot represents cell eccentricities from 102 cells from 2 experiments, in a range from 0 (round) to 1 (highly elliptical). The median, the lower and upper quartiles together with outliers are shown in the plot. The extraction of the property is described in section 8.4. The p-values are: $P < 8 \cdot 10^{-6}$ between FN=0.1μg and PLL, $P < .8$ (not significant) between FN=0.1μg and FN=1μg, $P < .18$ (not significant) between FN=1μg and FN=10μg, $P < .4$ (not significant) between FN=10μg and FN=50μg. **d)** Fluorescent (gray-scale, inverted) images (Paxillin), taken with the TIRF microscope (100X objective), representing FAs that fibroblasts form on given conditions (scale: 9.1924 pixels/μm). **e)** FA area (in μm^2) as a function of FN concentration. Each box-plot contains the FA data from 10 cells per experiment, a total of 590 FAs from 30 cells. The property is extracted from the Paxillin segmentation, imaged on a TIRF microscope, section 8.2. The median, the lower and upper quartiles together with outliers are shown in the plot. The p-values are: $P < .004$ between FN=0.1μg and FN=1μg, $P < .0002$ between FN=1μg and FN=10μg and $P < .5$ (not significant) between FN=10μg and FN=50μg. **f)** FA eccentricity as a function of FN concentration (range 0 to 1). Each box-plot contains the FA data from 10 cells per experiment, a total of 590 FA from 30 cells. The property is extracted from the Paxillin segmentation, imaged on a TIRF microscope, section 8.2. The median, the lower and upper quartiles together with outliers are shown in the plot. The p-values are: $P < 5 \cdot 10^{-13}$ between FN=0.1μg and FN=1μg, $P < .0001$ between FN=1μg and FN=10μg and $P < .0002$ between FN=10μg and FN=50μg. ***Significance levels:*** $* = P < .05$, $** = P < .01$, $*** = P < .001$ *and* ns = *not significant.*

9.2 Integrin activation promotes the alignment of F-actin in FAs

MEFs plated on different FN concentrations seem to develop distinctive F-actin organization in FAs where increased integrin activation promotes the alignment of F-actin in FAs. This conclusion can be drawn by comparing the anisotropy data across the chosen concentration conditions. The image analysis procedure is shown in Figure 9a), illustrating a MEF cell plated on FN = 50μg for demonstration. The raw data points from one (of three in total) executed experiments together with the binned data and the fitted trigonometric curves for every condition are shown in Figure 9b). The PLL sample could not be examined as FAs did not form and thus were impossible to segment. This means that this particular experiment lacks a control. By visually comparing the curves one can see the differences in anisotropy, as the amplitude of the curves increases with higher FN concentration. The three performed experiments show similar results and the trend is retained. The extracted amplitudes are shown in a plot Figure 9c).

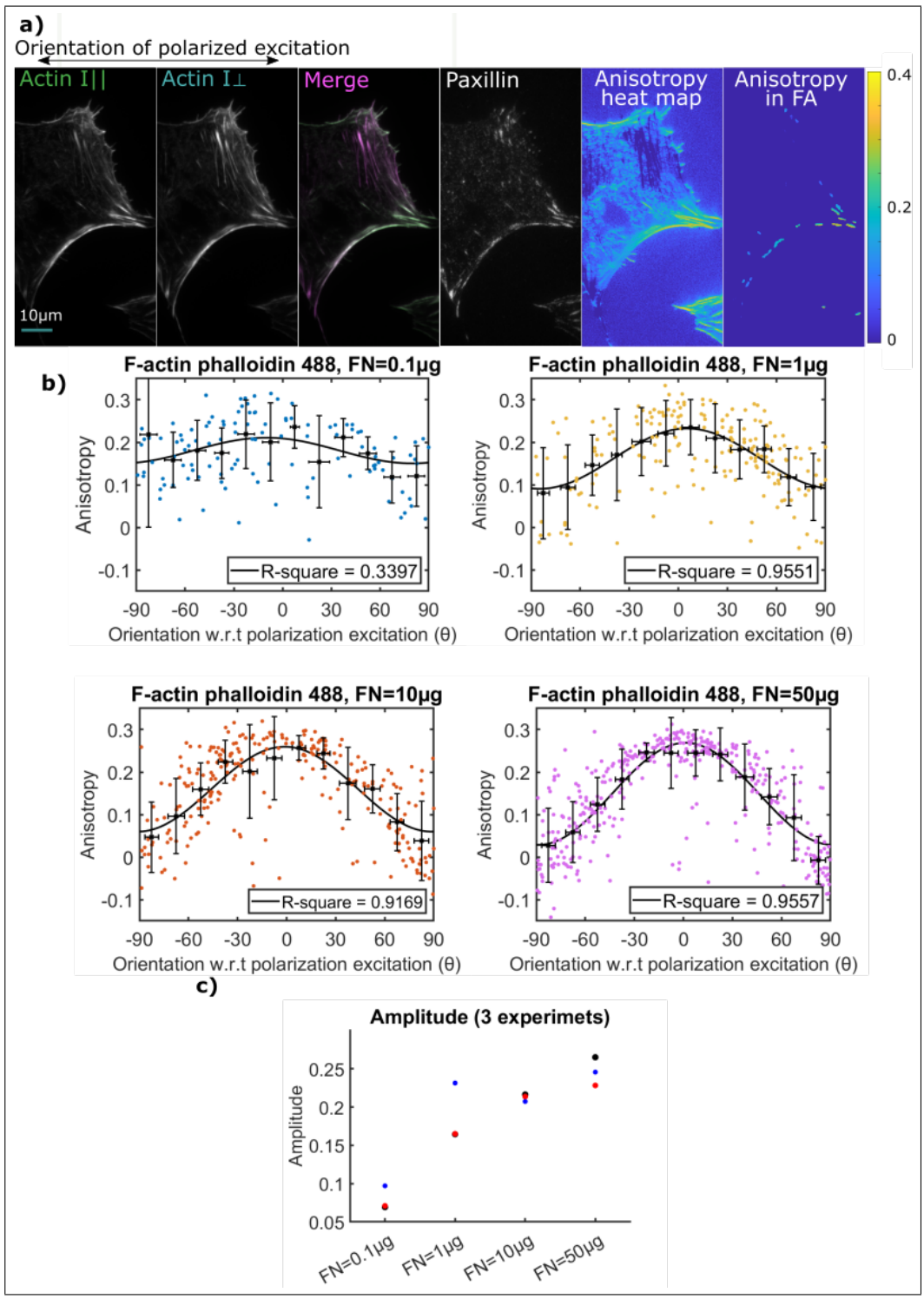
a)
Orientation of polarized excitation
Actin I||
Actin I⊥
Merge
Paxillin
Anisotropy heat map
Anisotropy in FA
10μm
0.4
0.2
0
b)
F-actin phalloidin 488, FN=0.1μg
R-square = 0.3397
F-actin phalloidin 488, FN=1μg
R-square = 0.9551
F-actin phalloidin 488, FN=10μg
R-square = 0.9169
F-actin phalloidin 488, FN=50μg
R-square = 0.9557
Anisotropy
Orientation w.r.t polarization excitation (θ)
c)
Amplitude (3 experimets)
Amplitude
FN=0.1μg
FN=1μg
FN=10μg
FN=50μg

Figure 9:

Figure 9: **Integrin activation promotes the alignment of F-actin in FAs**. **a)** MEF cell, plated on FN=50μg. From left to right: Fluorescent image, taken in TIRF mode (100X), of F-actin in the parallel channel (with respect to the orientation of polarized excitation). Fluorescent image, taken in TIRF mode (100X), polarized F-actin in the perpendicular channel. A merged image of the two respective channels where the parallel channel is green and the perpendicular is magenta-colored. Fluorescent image of paxillin taken in TIRF mode (100X), red channel. Anisotropy heat map created by using the method that is described in section 8.2, range 0-0.4. Anisotropy in FAs, see section 8.2, range 0-0.4. Scale: 9.1924 pixels/μm. **b)** FA anisotropy plotted as a function of FA long axis orientation with respect to the orientation of polarized excitation. The four plots correspond to the respective FN concentration. The raw data points are collected from one of the experiments (3 were made in total) and represent FAs from 10 cells per sample. The mean anisotropy values in 15$\circ$ bins together with the standard deviations for every bin (in both x and y) are plotted in black. The trigonometric function is fitted to the binned values and is shown in black. The legends display the goodness of fit represented as the R-square value. See section 8.2 for detailed description. **c)** The plot shows the amplitudes extracted from the fitted trigonometric functions from the three executed experiments (marked with respective color) for the four FN concentrations.

9.3 YAP response in fibroblasts is altered due to integrin activation

The YAP response in fibroblasts is influenced by the integrin activation. Fluorescent images, demonstrating YAP, F-actin, and the nuclear biomarker for the different concentration conditions are shown in Figure 10a). Additionally, the same figure shows the merge of all three channels together. The YAP nuclear/cytoplasmic ratios across the different FN concentrations are presented in a boxplot in Figure 10b). The cells plated on the control (PLL) condition have the lowest YAP ratio, where the YAP is mostly localized in the cytoplasm. According to the plot, the YAP response seems to exhibit a switch-like behavior on the FN=1μg condition as it drastically drops between the FN=0.1μg and FN=1μg and again increases with the raised FN concentration.

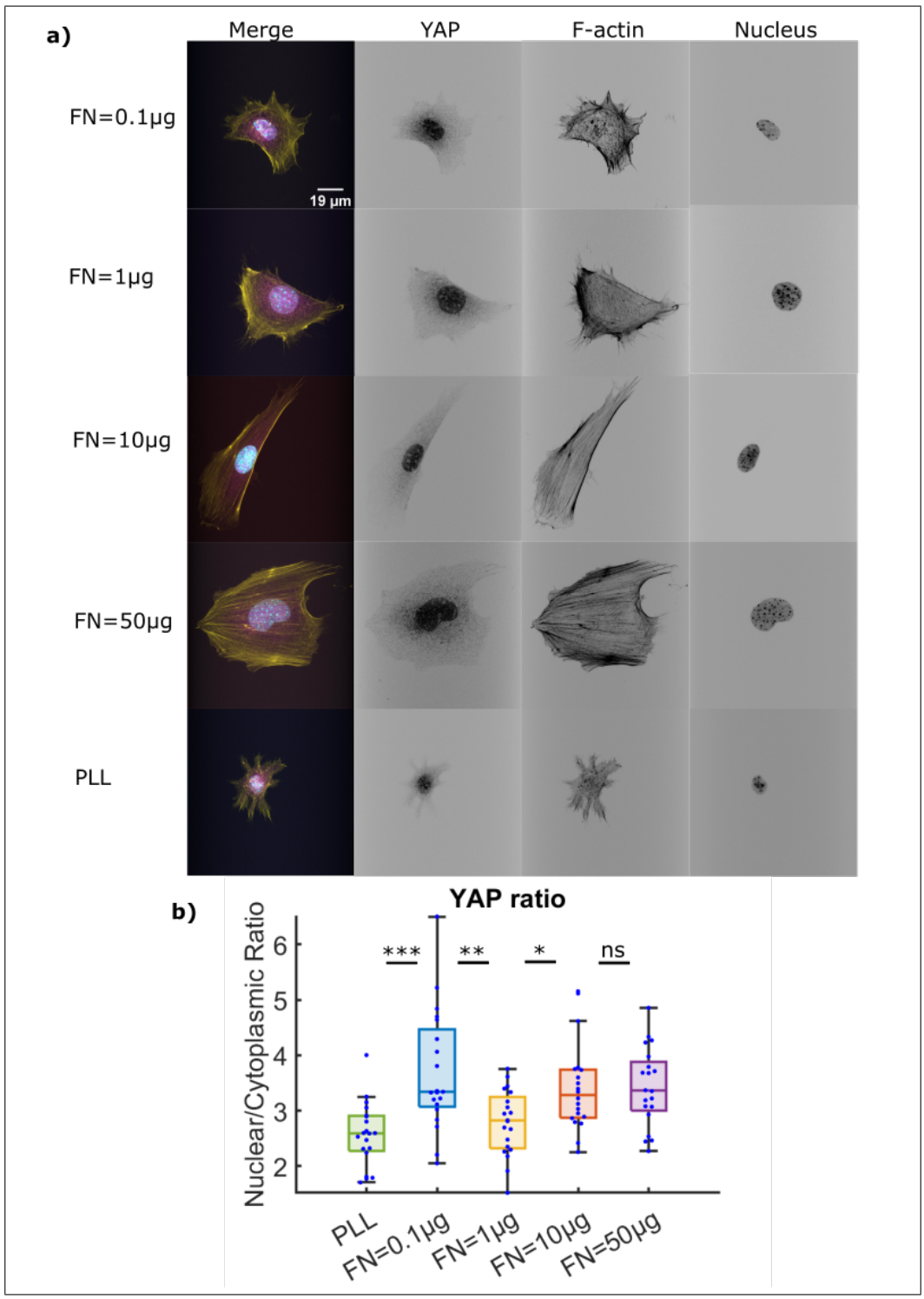
a)
Merge
YAP
F-actin
Nucleus
FN=0.1µg
FN=1µg
FN=10µg
FN=50µg
PLL
19 µm
b)
YAP ratio
Nuclear/Cytoplasmic Ratio
2
3
4
5
6
***
**
*
ns
PLL
FN=0.1µg
FN=1µg
FN=10µg
FN=50µg

Figure 10:

Figure 10: **YAP response in fibroblasts is altered due to integrin activation**. **a)** From left to right: Merged fluorescent images of the tree biomarkers: nucleus (cyan), YAP (magenta), and F-actin (yellow). Fluorescent (gray-scale, inverted) images of YAP, F-actin, and the nucleus. Scale: 8.1299 pixels/μm. The images are taken using the confocal (100X objective) microscope setup. **b)** YAP nuclear/cytoplasmic ratio as a function of FN concentrations. Each boxplot contains data from two experiments, 10 cells from each. The individual raw data points are illustrated as blue dots. The median, the lower and upper quartiles together with outliers are shown in the plot. The p-values were calculated using a Mann-Whitney U-test: $P < 1.8 \cdot 10^{-4}$ between PLL and FN=0.1μg, $P < .005$ between FN=0.1μg and FN=1μg, $P < .016$ between FN=1μg and FN=10μg, $P < .7$ (not significant) between FN=10μg and FN=50μg. ***Significance levels:*** $* = P < .05$, $** = P < .01$, $*** = P < .001$ *and* ns = *not significant.*

9.4 YAP activation and F-actin anisotropy in FAs are changing as a response to the restricted ability of FN remodeling and integrin activation

We hypothesized to see a difference in cell and FA morphology, YAP activation, and F-actin anisotropy in FAs as a response to inhibition of $\alpha_5\beta_1$ integrins and the restriction of FN remodeling. Here, we discuss the differences between chosen FN concentrations (FN=0.1μg and FN=10μg) and the respective cross-linked conditions (FN=0.1μg cl. and FN=10μg cl.) in terms of the previously stated parameters. The possible trends are not clear, as cells seem to react to the high and low FN concentration in different ways.

The fluorescent images, illustrating cell area and eccentricity for the cross-linked conditions are shown in Figure 11a), to the left. The cells plated on the FN=0.1μg cl. reveal a larger cell area compared to FN=0.1μg, while there is no significant difference between the FN=10μg and FN=10μg cl., see Figure 11b). The cell eccentricity does not change across the FN=0.1μg and FN=0.1μg cl conditions, but drops dramatically when comparing FN=10μg and FN=10μg cl, see Figure 11c).

The FA area does not significantly change when comparing between the normal and the cross-linked condition, see Figure 11d). The FA eccentricity is higher when the cells are plated on FN=0.1μg cl. compared to the FN=0.1μg, which implies that the FAs are more elongated on the cross-linked condition. However, the FAs are more circular on the FN=10μg cl. compared to the FN=10μg, see Figure 11e).

The merge of tree biomarkers (YAP - magenta, F-actin - yellow, and nucleus - cyan), together with three separate images illustrating each of the biomarkers for the cross-linked conditions are shown in Figure 11a), to the right. The YAP response does not seem to be triggered by the ability of cells to remodel the ECM. The YAP ratios, shown in Figure 11f), are not significantly altered between the normal and the cross-linked conditions, neither on FN=1μg or FN=10μg. However, there seems to be an increase on FN=10μg cl compared to respective FN=10μg.

In Figure 12a), the images of the paxillin (FA biomarker), are shown, illustrating FAs formed at the cross-linked FN conditions. The plots in Figure 12b) and 12c)) are communicating the F-actin organizational behavior in FAs on the cross-linked conditions as opposed to the original ones. The anisotropy of F-actin drops significantly in the cross-linked condition when a high amount of integrins is activated. The alignment of F-actin does not change when a low amount of integrins is activated.

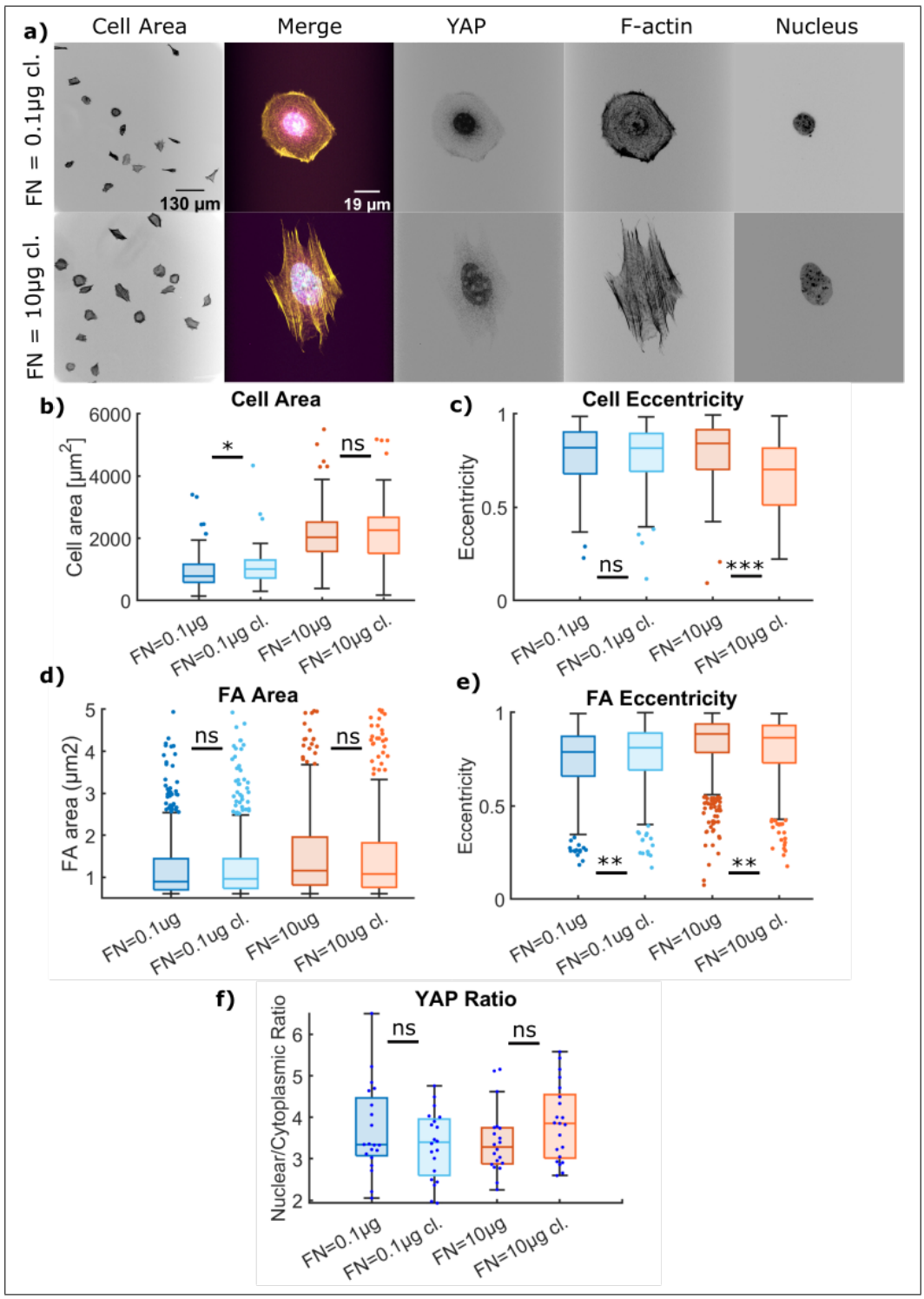
a)
Cell Area
Merge
YAP
F-actin
Nucleus
FN = 0.1µg cl.
FN = 10µg cl.
130 µm
19 µm
b)
Cell Area
Cell area [µm2]
6000
4000
2000
0
*
ns
FN=0.1µg
FN=0.1µg cl.
FN=10µg
FN=10µg cl.
c)
Cell Eccentricity
Eccentricity
1
0.5
0
ns
***
FN=0.1µg
FN=0.1µg cl.
FN=10µg
FN=10µg cl.
d)
FA Area
FA area (µm2)
5
4
3
2
1
ns
ns
FN=0.1ug
FN=0.1ug cl.
FN=10ug
FN=10ug cl.
e)
FA Eccentricity
Eccentricity
1
0.5
0
**
**
FN=0.1ug
FN=0.1ug cl.
FN=10ug
FN=10ug cl.
f)
YAP Ratio
Nuclear/Cytoplasmic Ratio
6
5
4
3
2
ns
ns
FN=0.1µg
FN=0.1µg cl.
FN=10µg
FN=10µg cl.

Figure 11:

Figure 11: **YAP response and the morphological properties are altered due to restricted ability of FN remodeling and integrin activation**. **a)** Images of cells plated on FN=0.1μg cl. and FN=10μg cl.. From left to right: fluorescent images of F-actin (scale: 1.834pixels/μm), taken in EPI mode (20X objective), merged image taken with confocal microscope setup (100X objective), composed of signals from tree biomarkers (YAP - magenta, F-actin - yellow and nucleus - cyan), followed by YAP, F-actin and nucleus gray-scale inverted images (scale: 8.1299 pixels/μm). **b)** Cell areas (in μm^2) as a function of normal FN versus cross-linked FN for two chosen concentrations FN=0.1μg and the FN=10μg. The data is presented as boxplots, where each contains cell areas of 102 cells from two experiments. The median, the lower and upper quartiles together with outliers are shown in the plot. The p-values were calculated using a Mann-Whitney U-test: $P < .03$ between FN=0.1μg and FN=0.1μg cl., and $P < .5$ (not significant) between FN=10μg and FN=10μg cl.. **c)** Cell eccentricity for the same conditions as in a), presented as boxplots with 102 data points in each. The median, the lower and upper quartiles together with outliers are shown in the plot. The p-values are: $P < .9$ (not significant) between FN=0.1μg and FN=0.1μg cl., and $P < 7 \cdot 10^{-7}$ between FN=10μg and FN=10μg cl..**d)** Focal adhesion area as a function of normal FN versus cross-linked FN for two chosen concentrations. Each boxplot contains FA areas collected from three experiments, 502 FAs in total. The median, the lower and upper quartiles together with outliers are shown in the plot. The Mann-Whitney U-test showed that there are no significant differences between the normal FN and the respective cross-linked condition. **e)** FA eccentricity as a function of normal FN versus cross-linked FN for two chosen concentrations. Each boxplot contains FA areas collected from three experiments, 502 FAs in total. The median, the lower and upper quartiles together with outliers are shown in the plot. According to the Mann-Whitney U-test, the p-values are: $P < .01$ between FN=0.1μg and FN=0.1μg cl., $P < .005$ between FN=10μg and FN=10μg cl.. **f)** YAP nuclear/cytoplasmic ratio for the two FN concentrations and the respective cross-linked conditions. Each boxplot contains data from two experiments (10 cells from each), 20 data points in total. The median, the lower and upper quartiles together with outliers are shown in the plot. The blue dots are representing the raw data points. According to the Mann-Whitney U-test, the differences between the original and cross-linked conditions for both concentrations are not significant. ***Significance levels:*** $* = P < .05$, $** = P < .01$, $*** = P < .001$ *and* ns = *not significant.*

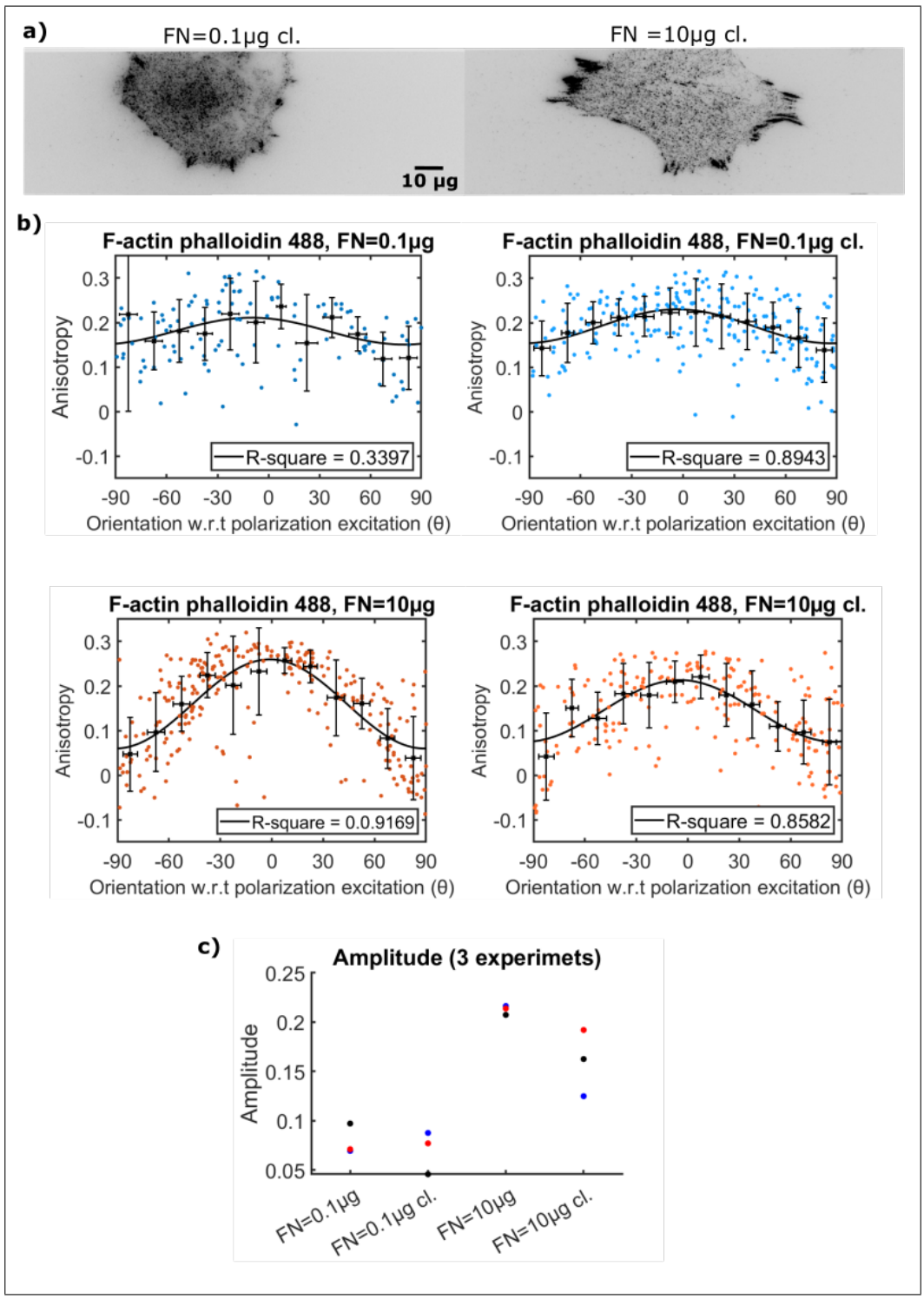
a)
FN=0.1µg cl.
FN =10µg cl.
10 µg
b)
F-actin phalloidin 488, FN=0.1µg
F-actin phalloidin 488, FN=0.1µg cl.
F-actin phalloidin 488, FN=10µg
F-actin phalloidin 488, FN=10µg cl.
Anisotropy
Orientation w.r.t polarization excitation (θ)
R-square = 0.3397
R-square = 0.8943
R-square = 0.0.9169
R-square = 0.8582
c)
Amplitude (3 experimets)
Amplitude
FN=0.1µg
FN=0.1µg cl.
FN=10µg
FN=10µg cl.

Figure 12:

Figure 12: **The alignment of F-actin in FAs is altered due to restricted ability of FN remodeling and integrin activation**. **a)** Fluorescent images of Paxillin (FA marker) taken in TIRF mode (100X objective). Scale: 9.1924 pixels/μm. The cells are plated on cross-linked FN (FN=0.1μg and FN=10μg). **b)** FA anisotropy plotted as a function of FA long axis orientation with respect to the orientation of polarized excitation. The plots correspond to two FN concentrations (FN=0.1μg and FN=10μg) and the respective cross-linked condition. The raw data points are collected from one of the experiments (3 were made in total) and represent FAs from 10 cells per sample. The mean anisotropy values in 15° bins together with the standard deviations for every bin (in both x and y) are plotted in black. The trigonometric function is fitted to the binned values and is shown in black. The legends display the goodness of fit represented as the R-square value. See section 8.2 for detailed description. **c)** Amplitudes from the three experiments (marked with a respective color), extracted from the fitted trigonometric functions. The difference between the mean amplitude of FN=0.1μg and FN=0.1μg cl. is 0.0091 and 0.0527 between the FN=10μg and FN=10μg cl..

10 Discussion

Alteration of FN concentration:

Cells increase in area when a larger amount of integrins become activated. They simultaneously become more polarized until a certain point (10μg/ml FN), after which they become again more circular. These features were compared across the two performed experiments (F-actin anisotropy and YAP response), to ensure similar cell morphology and control that the cells overall respond equally to conditions.

FAs become larger and more elongated due to increased integrin activation, simultaneously, the F-actin becomes more aligned in FAs. These findings possibly indicate that FA assembly is highly dependent on integrin activation. Higher FN concentrations grant a higher amount of integrin binding sites and consequently facilitate FA formation. This would also suggest that developed and polarized FAs promote the alignment of the F-actin structure.

One reason for the low R-square at FN = 0.1μg could be the less defined FAs that are forming and consequent imperfect segmentation, which might distort the extraction of the FA long-axis orientation and lead to a noisier data appearance. At other FN concentrations, the segmentation quality is improved, although some data points might be noise originated. It was mentioned earlier that the signal is a combination of the filament orientation and wobbling of the fluorescent probe and can not be decoupled. To invest the impact of wobbling an unconstrained dye could have been used. Though, as the trend is preserved and the phase of all trigonometric functions is located around zero degrees, the extracted amplitudes are a trustworthy measure of the organizational degree.

The YAP activation is high at 0.1μg/ml FN, drastically drops, and then gradually increases with raised FN concentration. The raise of YAP activation matches the F-actin organization trend, yet the behavior on low FN concentration does not. This pattern is possibly influenced by an interplay of different activation pathways, where the influence of the Hippo cascade and mechanotransduction are varying throughout the conditions. Different environments may induce the dominance or

inhibition of the respective pathways. Perhaps, when integrins are less activated, in absence of appropriate ligands, the mechanotransduction signaling pathway is inactivated and is YAP predominantly regulated by the canonical Hippo pathway. It could be, that when access to RGD motifs and synergy sites is gradually increased, the mechanotransduction pathway dictates the regulation. Further experiments are needed to confirm this assumption.

In highly spread cells with large cell areas, sufficient amounts of YAP could have resided beyond the cytoplasmic segmentation. To improve the quality of the measurement one could have taken the property of cell area into account, by for example adjusting the thickness of the doughnut-shaped segmentation accordingly.

Restriction of ECM remodeling and ligand accessibility:

The cell area appears to slightly increase when the number of activated integrins is low and does not change when high. On 0.1μg/ml FN the eccentricity does not change between the conditions, however, on 10μg/ml FN cross-link cells polarize less, compared to the original FN coating. Perhaps, the cross-link at low FN concentrations does not impact the spreading and polarization of cells as the access to integrin-binding ligands is insufficient. On the other hand, when the access is increased, the impact of cross-linking is distinguishable, as fibroblasts are not able to polarise after restricted matrix remodeling. Possibly, cross-linked FN inhibits the directional persistence of fibroblasts.

FA area does not change between the conditions in both cases, though the FA eccentricity is higher on 0.1μg/ml FN cl. opposed to 0.1μg/ml FN and lower on 10μg/ml FN cl. opposed to 10μg/ml FN. There is also a smaller relative change in F-actin organization in the case of 0.1μg/ml FN compared to 10μg/ml FN. The F-actin organization is sufficiently more disorganized on the cross-linked condition when a high amount of integrins is activated. When a cell moves in a certain orientation, it needs to remodel the matrix accordingly. As the remodeling is restricted, FAs may not be able to polarise and assemble in an oriented manner. Further, that may imply disorganization of actin filaments. Here, it would be interesting to see how the integrins are organized. Again, the FA structure is more affected on high

concentrations of FN compared to low, which is influenced by the overall ligand accessibility. These results, perhaps, also depend on what kinds of integrins get activated. If $\alpha_5\beta_1$ integrins can not attach to both the RGD motif and the synergy site because of the cross-linking, the properties of FAs and mechanosensing may be altered.

YAP activation is slightly altered on the cross-linked FN conditions, even though the changes are not significant. A potential explanation for that could be inhibition of the mechanotransduction signaling pathway, as the mechanosensing and FA structural organization are affected. Most likely, another signaling pathway, for example, the Hippo cascade, is triggered. The possible inhibition of integrins $\alpha_5\beta_1$ activation could also affect the mechanosensing. Additional experiments are required to draw any conclusions.

11 Conclusions

The goal of this project was to extend the knowledge of the mechanotransduction pathway and its regulation of YAP. The mechanosensing was modulated by modifying the FN coating, which controls the integrin activation and consequently affects the FA morphology together with the organization of F-actin in FAs. Our findings provide a foundation for further experiments in the field and suggest that YAP response can be triggered by integrin activation. However, the mechanotransduction and the Hippo signaling pathways need to be decoupled before drawing any conclusions. Possibly, the two pathways have different impacts, when the integrins are activated or inhibited. We suggest that integrin activation favors the alignment of F-actin. Possibly when the F-actin is aligned, it can apply forces on the nucleus, stimulating the inflow of YAP by opening the nuclear pores, see Figure 13.

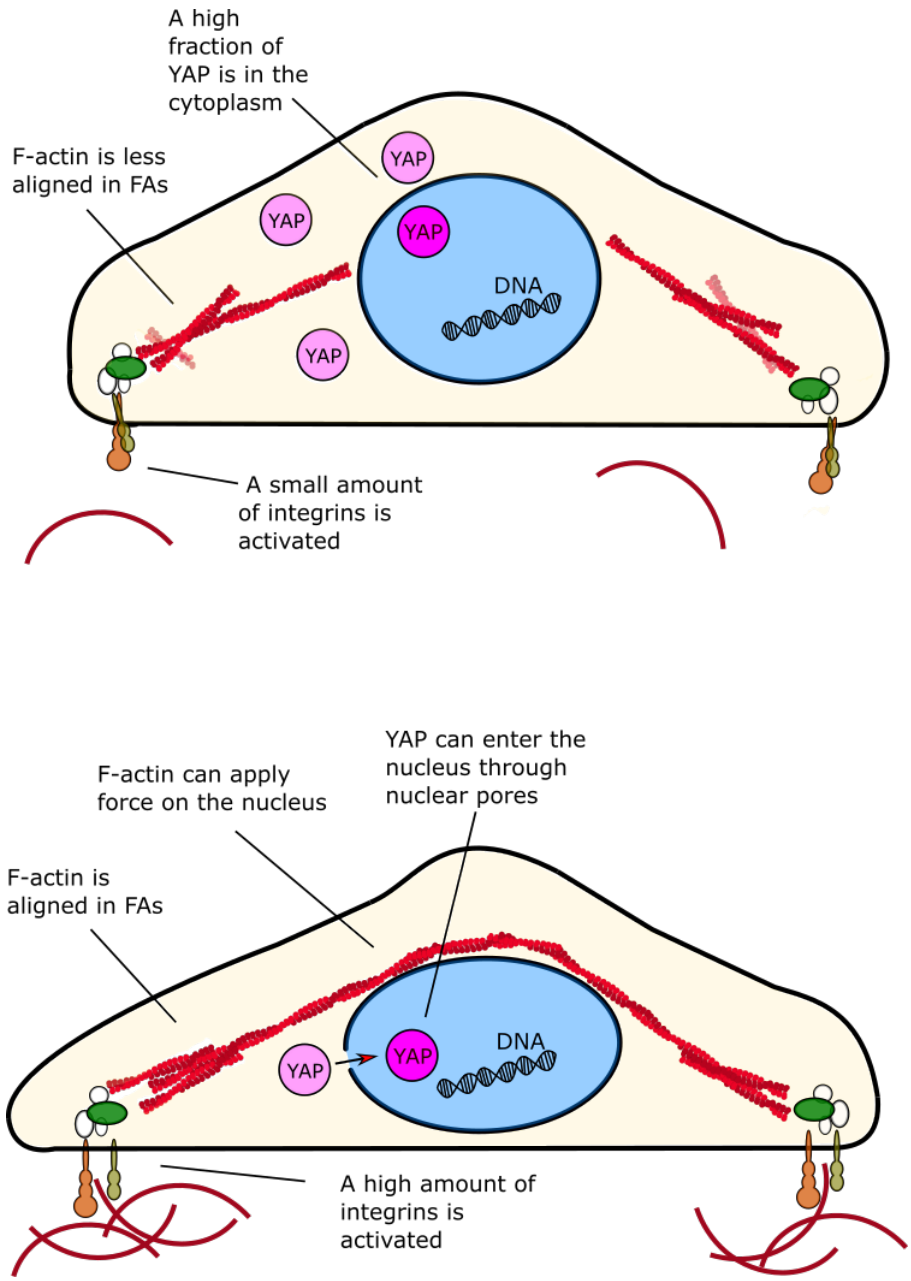

Figure 13: **A model that describes a possible mechanotransduction pathway that can regulate YAP activation.**

12 Future prospective

Firstly, additional experiments would be necessary before converting the assumptions into conclusions. We would need to assure that fibroblasts are not secreting high amounts of FN in four hours, which could influence the conditions. This could be achieved by staining the human and mouse FN respectively. To further investigate the effect of cross-linking, we would need to test whether the activation of $\alpha_5\beta_1$ integrins is restricted. That could be done by immunostaining or transfecting the integrins $\alpha_5\beta_1$ and $\alpha_v\beta_3$. Further, we would need to separate the effects of the Hippo signaling and the mechanotransduction pathways.

Secondly, it would be interesting to further explore the couplings between YAP activation and the actin cytoskeleton. One possible way is to model the anisotropy in locations other than FAs, for example in the actin structures that cover and apply force on the nucleus from above. Correlating these modulations with the YAP localization and nuclear deformation could reveal curious interactions. Nuclear deformation is an interesting topic per se. Another approach could be involving the integrin organization and tilting under the same condition. That would provide information about the directional features as well as actin and integrin dependence. Lastly, the usage of superresolution microscopy techniques would enable structural investigations on a yet finer scale.

References

[1] "Cancer." [Online]. Available: https://www.who.int/news-room/fact-sheets/detail/cancer

[2] A. Totaro, T. Panciera, and S. Piccolo, "Yap/taz upstream signals and downstream responses," *Nature Cell Biology*, vol. 20, 07 2018.

[3] S. Dupont, "Role of YAP / TAZ in cell-matrix adhesion-mediated signalling and mechanotransduction," *Elsevier*, vol. 343, pp. 42–53, 2016.

[4] V. Swaminathan, J. Kalappurakkal, S. Mehta, P. Nordenfelt, T. Moore, N. Koga, D. Baker, R. Oldenbourg, T. Tani, S. Mayor, T. Springer, and C. Waterman-Storer, "Actin retrograde flow actively aligns and orients ligand-engaged integrins in focal adhesions," *Proceedings of the National Academy of Sciences*, vol. 114, pp. 10 648–10 653, 10 2017.

[5] B. Hoffman, C. Grashoff, and M. Schwartz, "Dynamic molecular processes mediate cellular mechanotransduction," *Nature*, vol. 475, pp. 316–23, 07 2011.

[6] X. Trepat, Z. Chen, and K. Jacobson, "Cell migration," *Comprehensive Physiology*, vol. 2, pp. 2369–2392, 10 2012.

[7] F. Martino, A. R. Perestrelo, V. Vinarský, S. Pagliari, and G. Forte, "Cellular mechanotransduction: From tension to function," *Frontiers in Physiology*, vol. 9, p. 824, 2018.

[8] P. Cramer, "Organization and regulation of gene transcription," *Nature*, vol. 573, pp. 1–10, 08 2019.

[9] J. Z. Kechagia and J. Ivaska, "Integrins as biomechanical sensors of the microenvironment," *Nature Reviews Molecular Cell Biology*. [Online]. Available: http://dx.doi.org/10.1038/s41580-019-0134-2

[10] Y. Mao and J. E. Schwarzbauer, "Accessibility to the fibronectin synergy site in a 3d matrix regulates engagement of $\alpha_5\beta_1$ versus $\alpha_v\beta_3$ integrin receptors,"

Cell Communication & Adhesion, vol. 13, no. 5-6, pp. 267–277, 2006, pMID: 17162669. [Online]. Available: https://doi.org/10.1080/15419060601072215

[11] B. Geiger, J. Spatz, and A. Bershadsky, "Geiger b, spatz jp, bershadsky adenvironmental sensing through focal adhesions. nat rev mol cell biol 10: 21-33," *Nature reviews. Molecular cell biology*, vol. 10, pp. 21–33, 02 2009.

[12] J. Seo and J. Kim, "Regulation of hippo signaling by actin remodeling," *BMB reports*, vol. 51, 01 2018.

[13] C. GM., *The Cell: A Molecular Approach. 2nd Edition*. Sinauer Associates, Incorporated, 2000. [Online]. Available: https://www.ncbi.nlm.nih.gov/books/NBK9908/

[14] A. Pocaterra, P. Romani, and S. Dupont, "Yap/taz functions and their regulation at a glance," *Journal of Cell Science*, vol. 133, p. jcs230425, 01 2020.

[15] D. Missirlis, T. Haraszti, H. Kessler, and J. Spatz, "Fibronectin promotes directional persistence in fibroblast migration through interactions with both its cell-binding and heparin-binding domains," *Scientific Reports*, vol. 7, 06 2017.

[16] E. Cowles, L. Brailey, and G. Gronowicz, "Integrin-mediated signaling regulates ap-1 transcription factors and proliferation in osteoblasts," *Journal of biomedical materials research*, vol. 52, pp. 725–37, 01 2001.

[17] D. Mazia, G. Schatten, and W. Sale, "Adhesion of cells to surfaces coated with polylysine. applications to electron microscopy," *The Journal of cell biology*, vol. 66, pp. 198–200, 08 1975.

[18] A. M. López-Colomé, I. Lee, R. Benavides-Hidalgo, and E. López, "Paxillin: A crossroad in pathological cell migration," *Journal of Hematology Oncology*, vol. 10, 02 2017.

[19] D. Axelrod, "Chapter 9 total internal reflection fluorescence microscopy," in *Fluorescence Microscopy of Living Cells in Culture Part B. Quantitative Fluorescence Microscopy—Imaging and Spectroscopy*, ser. Methods in Cell

Biology, D. L. Taylor and Y.-L. Wang, Eds. Academic Press, 1989, vol. 30, pp. 245–270. [Online]. Available: https://www.sciencedirect.com/science/article/pii/S0091679X08609826

[20] S. Ghosh, S. Saha, D. Goswami, S. Bilgrami, and S. Mayor, "Chapter sixteen - dynamic imaging of homo-fret in live cells by fluorescence anisotropy microscopy," in *Imaging and Spectroscopic Analysis of Living Cells*, ser. Methods in Enzymology, P. Conn, Ed. Academic Press, 2012, vol. 505, pp. 291–327. [Online]. Available: https://www.sciencedirect.com/science/article/pii/B9780123884480000243

[21] J. Lakowicz, *Principles of Fluorescence Spectroscopy*, 01 2006, vol. 1.

[22] A. L. Mattheyses, M. Kampmann, C. E. Atkinson, and S. M. Simon, "Fluorescence anisotropy reveals order and disorder of protein domains in the nuclear pore complex," *Biophysical Journal*, vol. 99, no. 6, pp. 1706–1717, 2010. [Online]. Available: https://www.sciencedirect.com/science/article/pii/S0006349510008489

[23] C. A. Valades Cruz, H. A. Shaban, A. Kress, N. Bertaux, S. Monneret, M. Mavrakis, J. Savatier, and S. Brasselet, "Quantitative nanoscale imaging of orientational order in biological filaments by polarized superresolution microscopy," *Proceedings of the National Academy of Sciences*, vol. 113, no. 7, pp. E820–E828, 2016. [Online]. Available: https://www.pnas.org/content/113/7/E820

[24] MATLAB, *version 9.8.0.1451342 (R2020a) Update 5*. Natick, Massachusetts: The MathWorks Inc., 2010.

[25] A. Elosegui-Artola, I. Andreu, A. E. Beedle, A. Lezamiz, M. Uroz, A. J. Kosmalska, R. Oria, J. Z. Kechagia, P. Rico-Lastres, A.-L. Le Roux, C. M. Shanahan, X. Trepat, D. Navajas, S. Garcia-Manyes, and P. Roca-Cusachs, "Force triggers yap nuclear entry by regulating transport across nuclear pores," *Cell*, vol. 171, no. 6, pp. 1397–1410.e14, 2017. [Online]. Available: https://www.sciencedirect.com/science/article/pii/S0092867417311923

13 Annex

13.1 Rotational diffusion

Before performing anisotropy experiments, the microscope setup was tested to sense the effect of rotation diffusion on the anisotropy. For that, the same concentration of fluorescein was dissolved in a series of glycerol-water mixtures with increasing viscosity. The solutions were imaged with a laser (488nm) in EPI mode using the same camera and PB as for the later anisotropy measurement. The measurement is G-factor corrected. The problem with using the TIRF mode would be the eventual immobilized dye particles on the bottom of the glass surface. The expected result is an increase in anisotropy in viscous solutions due to the restricted rotational diffusion of fluorophores. [20]

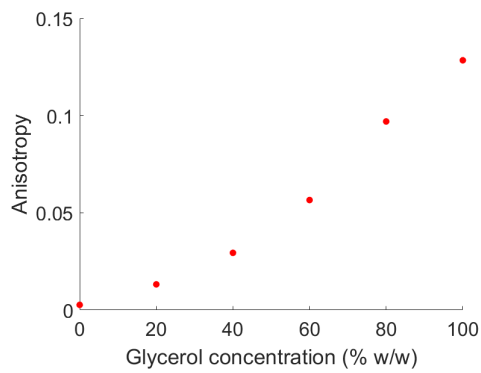

Figure 14: Anisotropy of FITC solution plotted as a function of the viscosity of the solvent (glycerol to water ratio).

13.2 SiR-actin

In the main experiments, the f-actin is stained with Phalloidin 488, which has a dipole moment that is oriented along the actin fibers. To visualize the meaning of

that, another experiment was performed, where another dye, SiR, was used. SiR attaches to the f-actin in such a way, so that the dipole moments of the dye are oriented perpendicularly with respect to the actin fibers [4]. The anisotropy plot is shown in Figure 15.

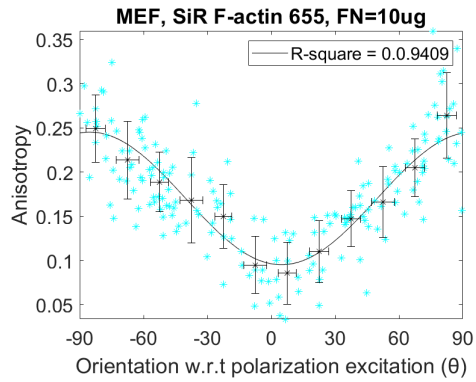

Figure 15: Anisotropy plot of SiR F-actin in FAs. The light blue points represent the raw data points from 10 cell images. The mean anisotropy values in 15° bins together with the standard deviations for every bin (in both x and y) are plotted in black. The trigonometric function is fitted to the binned values and is shown in black. The legends display the goodness of fit represented as the R-square value.